On the Separation of Enantiomers by Drift Tube Ion Mobility Spectrometry

Roberto Fernández-Maestre,[1,2] * *and Markus Doerr* [3]

[1] Departamento de Quimica, Campus de San Pablo, Universidad de Cartagena, Cartagena, Colombia.
[2] National Research Nuclear University MEPhI (Moscow Engineering Physics Institute), Kashirskoe sh. 31, Moscow, 115409, Russia. *rfernandezm@unicartagena.edu.co
[3] Universidad Industrial de Santander, Cra 27 Calle 9, Bucaramanga, Colombia. mhodoerr@uis.edu.co

ABSTRACT

Racemic mixtures of twelve common α-amino acids and three chiral drugs were tested for the separation of their enantiomers by drift tube ion mobility spectrometry (IMS)-quadrupole mass spectrometry (QMS) by introducing chiral selectors into the buffer gas of the IMS instrument. (R)-α-(trifluoromethyl) benzyl alcohol, (L)-ethyl lactate, methyl (S)-2-chloropropionate, and the R and S enantiomers of 2-butanol and 1-phenyl ethanol were evaluated as chiral selectors. Experimental conditions were varied during the tests, including buffer gas temperature, concentration and type of chiral selectors, analyte concentration, electrospray (ESI) voltage, ESI solvent pH, and buffer gas flow rate. The individual enantiomers yielded the same drift times and the racemic mixtures could not be separated as opposed to a previously report (Dwivedi et al. *Anal. Chem.* 2006, *78*, 8200). Energy calculations of the chiral selector –ion interactions showed that these separations are unlikely using 2-butanol as a chiral selector but they might be theoretically feasible depending on the chiral selector nature and the type of enantiomers. Several plausible explanations for not succeeding were analyzed. A critical review of previously claimed enantiomer separations by drift-tube IMS-MS is presented and recommendations for potential enantiomer separations by IMS are proposed.

Keywords: enantiomer separation, 2-butanol, theoretical calculations, racemic mixtures, ion mobility spectrometry

Enantiomers are stereoisomers that are mirror images of each other. They are important because of their environmental impact and economic, clinical, industrial, and biochemical significance. The most widely accepted model for stereoselectivity is the three-point interactions model, which calls for three-point interactions between receptor and substrate. [1] In this model, stereochemical differences in biological activities are due to differential binding of enantiomers to a common site on a receptor surface. To distinguish between enantiomers, the receptor must have three non-equivalent binding sites. Chiral discrimination occurs when one isomer can simultaneously interact with all sites whereas the other only interacts with two sites. [2,3]

Because enantiomers have such a similar structure, they are difficult to analyze, yet their separation and purification are important in the pharmaceutical industry. Very often, one enantiomer of chiral drugs, the eutomer, is more active than the other, the distomer. The distomer may be inert or even toxic.

The most common analytical method for the analysis and purification of enantiomers is chromatography. Enantiomers can be separated using a stereoselective stationary phase if one enantiomer is more attracted to the phase.[4] The development of rapid methods for enantiomers has been investigated because traditional methods for the separation of these compounds, such as HPLC and gas chromatography, are limited by long sample preparation and analysis times[5] and the lack of enough resolution and sensitivity.[6] Mass spectrometry (MS) is the most widespread analytical method used for the rapid determination of the purity of chiral compounds. MS is not used as a separation technique, but as an indirect probe of chirality. Here, enantiomers are not physically separated, but rather the difference in fragmentation patterns when the enantiomers are subjected to collisions with stereoselective agents is used to distinguish and even quantify enantiomers. For example, diastereomeric adducts of enantiomers with chiral host molecules, such as cyclodextrins (CDs) and crown ethers were investigated in single-stage MS experiments.[7] It is clear from this and other examples that MS is not an enantiomeric separation technique, but rather diastereomeric.[8] MS methods for chiral recognition are reviewed by Wu et al.[9] MS methods have several limitations including the requirement of enantiopure reference compounds, cumbersome calibration, non-standard instrument modifications, theoretical modeling of the ion fragmentation patterns, and compound-dependent enantiomeric selectivity.[10]

Another rapid analytical method that has been used for enantiomer separations is ion mobility spectrometry (IMS). IMS enantiomer separations can be fast, sensitive, and inexpensive because IMS spectra can be obtained in less than a minute, concentrations down to nmol per liter can be detected, and the instrumentation does not require high-cost vacuum pumps given that IMS is an atmospheric pressure technique. IMS separates gas-phase ions based on their size to charge ratio. IMS has been used for the separation and analysis of stereoisomers on stand-alone instruments or coupled to chromatography and mass spectrometry instruments. [11]

The separation and analysis of enantiomers by IMS has been questionable. IMS was first applied to enantiomer separation by Dwivedi *et al.* in 2006. They reported the separation of racemic mixtures of amino acids by introducing (S) and (R)-2-butanol chiral selectors in the buffer gas and suggested that the enantiomer with the weaker interaction energy with the chiral selector would drift faster than the other, leading to chiral separation. [12] Karas patented this idea and claimed the separation of fluoxetine enantiomers using chiral 2-butanol.[13] These enantiomer separations have not been reproduced in commercial IMS instruments at lower pressures,[6] or at atmospheric pressures. Herbert Hill, IMS group research director at Washington State University (USA) in a comment to reference 12, sent to Analytical Chemistry Journal (2022), concluded that the enantiomer separation reported was most likely due to instrumental artifacts, small variations in environmental factors and results overinterpretation. Unsuccesful experiments seeking to separate enantiomers included the studies of several graduate students of this research group, including the author of this paper and Roscioli (2012).[14] In Roscioli´s study, methionine and methyl α-glucopyranoside enantiomers were tested for separation with (S) and (R)-2-butanol into the buffer gas of an ESI-IMS-TOF-MS. These were the same reagents used by Dwivedi.[12] They concluded that the separation of enantiomers with chiral modifiers was not possible using Dwivedi´s experimental protocol.[14]

Additional reported IMS chiral separations have only been applied to the resolution of diastereomers, common in the literature because they have different physical properties in contrast to enantiomers and, therefore, are easier to separate.[15]

Collisions of chiral ions and molecules were used to study the influence of chirality on the ion-molecule complexes formed and their fragmentation pattern and yield. Kulyk *et al.* (2017) reported the study of 0.1–10.0 eV low-energy collisions of L- and D-protonated enantiomers of phenylalanine, tryptophan, and methionine with (R)- and (S)-2-butanol, and (S)-1-phenylethanol chiral selector targets. They found that ion-molecule complex formation followed by dissociation was independent of the chirality of targets and ions; the fragment yield was also independent.[10] With a higher collision energy, equivalent results were obtained.[16] In a similar investigation, CID of proton-bound adducts of tryptophan and 2-butanol indicated that the heterochiral adduct was more stable in low-energy collisions with argon than the homochiral adduct.[17] In another study, enantiomers of phenylalanine, tryptophan, and methionine were used to form non-protonated adducts with enantiomers of 1-phenylethanol. The experimental results showed no influence of chirality on the adduct fragmentation upon collisions with Ar. Calculations showed a difference in the Gibbs energies of only ~0.5 kcal/mol between the formation of homochiral and heterochiral adducts of Met and Try and no difference for those of Phe.[18] However, this study did not report statistical data to determine if the observed differences in the Gibbs energies were significant.

The investigations on spectroscopy and photophysics of clusters of enantiomeric species provide insights into the IMS enantiomer separation with chiral selectors. Zehnacker (2014) conducted studies in spectroscopy and photophysics of chiral molecules or protonated ions, and their weakly bound complexes, isolated in the gas phase in jet-cooled conditions. She concluded that the ancillary interactions responsible for chiral recognition, such as OH…π or CH…π, would be blurred at room temperature.[19] Ion mobility experiments at higher temperatures would be even more blurred.

To date, most IMS enantiomer separations depend on the formation of chiral non-covalent diastereomeric complexes, where the D- or L- analyte ions complex with other chiral molecules using transition metal cations.[6] When reviewing the seven studies cited, there were no enantiomer separations by only injecting a chiral selector (Table S1). Therefore, one report claims IMS enantiomer separation [12] while others show the failure of these experiments[14] or their unsuitability to single collision conditions [10,16,18] because thousands of ion-chiral selector collisions are found in the traditional IMS tube.[20] Because of the inconsistent results of previous gas-phase IMS enantiomer separations,[12] difficulties on their implementation,[14] and their basis,[19] drift-tube IMS-QMS was used and energy calculations were made to study the viability of enantiomer separations by introduction of buffer gas chiral selectors.

EXPERIMENTAL SECTION

Instrumental setup. Experiments were performed using an electrospray-ionization atmospheric-pressure ion mobility spectrometer interfaced through a 40-μm pinhole to a quadrupole mass spectrometer (Figure S1) at Washington State University (WA, USA) in 2009. The IMS instrument was built at WSU and a full description is given elsewhere.[21] The

instrument was equipped with an electrospray ionization (ESI) source and a drift tube. The tube consisted of desolvation and drift regions in positive mode and separated by a Bradbury-Nielsen-type ion gate. Typical operating parameters were: ESI flow, 3 µL min^{-1}; reaction region length, 7.5 cm; drift tube length, 25.0 cm; ESI voltage, 15.6 kV; first ring voltage, 12.12 kV; gate voltage, 10.80 ± 0.01 kV; gate closure potential, ±40 V; gate pulse width, 0.1 ms; scan time, 35 ms; pressure, 680-710 Torr; buffer gas, nitrogen; buffer gas temperature, 150 ± 2 ˚C; buffer gas flow, 1 liter min^{-1}.

Materials and reagents. Pure chiral analytes were purchased including alanine, arginine, asparagine, atenolol, histidine, lysine, methionine, penicillamine, phenylalanine, serine, threonine, tryptophan, tyrosine, valine, and valinol, and enantiomers of ethyl lactate, methyl-2-chloropropionate, α-(trifluoromethyl) benzyl alcohol, 1-phenyl ethanol, and 2-butanol as chiral selectors (Sigma-Aldrich, St. Louis, MO, USA). These chemicals were ACS reagent grade and their purities ≥98% (structures in Figure S2).

Sample and chiral selector introduction. Liquid samples were electrosprayed at a flow rate of ~3 µl min^{-1} into the drift tube. The liquid chiral selectors were injected into the buffer gas line using a T-junction at ~150 °C before the buffer gas heater (Figure S1).

Identification of compounds. Analytes were identified by comparing their *m/z* signal in mass spectrometry with the molecular weight of their protonated molecules or clusters. Furthermore, the reduced mobilities of the protonated analytes were compared with those in the literature. Additionally, selected ion monitoring-IMS (SIM-IMS) was performed on the analyte peaks and their clusters to identify the peaks in the IMS spectrum.

Instrument calibration. Under certain conditions, the product of an ion reduced mobility, K_0, and its drift time is constant. This fact allows the reduced mobility of ions to be calculated from that of a calibrant, $K_{0,c}$, the calibrant drift time, c_t, and the analyte drift time under the same conditions, d_t:

$$K_0 = K_{0,c} \frac{c_t}{d_t} \quad (1)$$

2,6-Di-tert-butylpyridine was used as a calibrant.

Experiments performed

The following conditions of the IMS instrument and samples were changed to study the effect on enantiomer separation:

- Stability of the mobilities of valine enantiomers with time: to rule out a difference in mobility between the enantiomers due to pressure changes or changes in other instrumental parameters when switching from one enantiomer to another (Section 1, Results and Discussion).
- Chiral selector concentration in the buffer gas: because it changes the interaction extent with the ions (Section 2, Results and Discussion).
- Analyte concentration: to check the effect of analyte to chiral selector concentrations ratio on the experiments (Section 3, Results and Discussion).

- Buffer gas temperature: because temperature affects the analyte ion-chiral selector interaction (Section 2, Results and Discussion).
- Chiral selector nature: because the interaction strength depends on the chiral selector structure (Section 4, Results and Discussion).
- ESI voltage and ESI solvent acidity, and proportions of D- and L- enantiomers in the racemic mixtures: to evaluate a possibile racemization due to solvent conditions or drift voltage (Section 5, Results and Discussion)

Computational Studies. The formations of complexes between (S)-2-butanol and protonated (R,S)-atenolol, (R,S)-serine and (R,S)-valinol in the gas phase were investigated. Atenolol was protonated at the isopropylamine nitrogen atom, and serine and valinol at the amine group.

We performed a search of the conformational space to identify representative structures. First, the CREST program was used to find low-energy conformers.[22] Structures were selected within a window of 9 kcal/mol. To improve the sampling of the conformational space, the simulation times were increased from their default values using the semi-empirical tight-binding method GFN2-xTB.[23] Then, all structures were reoptimized using the B97-3c DFT method.[24] Here, a triple-zeta basis was applied and the D3 dispersion correction was included. Next, duplicated structures were eliminated using DockRMSD.[25]

Single point energy calculations were performed on structures with the lowest free energy using the ωB97X-V density functional[26] and the def2-QZVP basis set[27] to minimize the superposition error. We also performed analyses using the complete ensembles of structures obtained after B97-3c minimization. However, the results were very similar to those obtained with only the lowest energy structure.

All DFT calculations were performed with ORCA, version 4.2.1.[28] To speed up the calculations with the ωB97X-V functional, the RIJ-COSX approximation was applied.[29] Thermodynamic quantities were calculated using the geometries and vibrational frequencies obtained at the B97-3c level of theory at 423K, consistent with experimental conditions.

Results and Discussions

MS spectra (500 scans per spectrum) and mobility spectra (at least 250 scans per spectrum) were acquired after stabilizing the chiral selector concentration for at least one hour and when the peak height ratio of the protonated analyte to the analyte-chiral selector cluster was reproducible from one spectrum to the next, indicating stable conditions in the drift tube. The reproducibility of the reduced mobilities was <2%, calculated as the relative standard deviation of the reduced mobilities of five different samples with the same concentration prepared independently and analyzed on different days. The repeatability of the reduced mobilities was <0.5%, calculated as the relative standard deviation of the reduced mobilities of five or more consecutive analyses of the sample (1600 scans each).

1. Stability of the mobilities of valine enantiomers with time

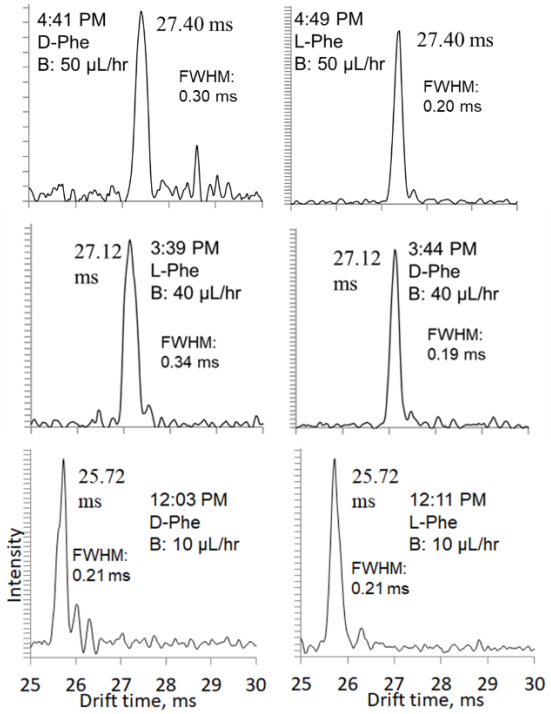

Figure 1. IMS spectra of the enantiomers D- and L- of phenylalanine (Phe) when 10, 40, and 50 µL/hr of 2 butanol (B) was introduced in the buffer gas at 150°C. The time when the spectra was taken is shown. FWHM: full-width at half-maximum. With these data, resolving power was calculated in Table S2.

The stability of the mobilities of valine enantiomers was monitored over time while (S)-2-butanol was injected into the buffer gas to rule out a difference in mobility between the enantiomers of the same compound due to pressure changes or changes in other instrumental parameters when changing from one enantiomer to another. In several experiments, the racemic mixtures could not be separated nor did the enantiomers show different drift times (Table 1, Figures 1 and S3). In one experiment (Appendix 1), the enantiomers produced different drift times, although not enough to separate a racemic mixture; this experiment could not be reproduced.

2. Chiral selector concentration/buffer gas temperature and enantiomer separation

Table 1. Racemic mixtures that could not be separated and individual enantiomers whose drift times were not significantly different, with several chiral selectors (62 different unsuccessful experiments, >4000 analyses). The analyte concentration was 500 µM and the buffer gas temperature was 150°C, unless otherwise specified. Data were obtained switching between one enantiomer to the other. See a detailed explanation of this table below. Additional unsuccessful experiments are detailed in section 5.

Chiral selector	**Analyte [Concentrations of chiral selector in the buffer gas in mmol m^{-3}]**
(R)-1-phenyl ethanol	D- and L-: Asn, Met, Phe: [5.3] and [2.1, 4.2, 6.3]
(S)-1-phenyl ethanol	D- and L-Phe [0.42, 0.63]; R and S-Atenolol[5.3]
(R)-2-butanol	D- and L-: Ser [6.9];[a] Met [0.69], [4.8, 6.2, 7.6, 14], [3.4, 5.5, 7.6], and [1.4, 2.8, 4.1, 5.5, 6.9, 8.3]; valinol, Val [6.8] (4 experiments); Tyr [6.1]; R and S-Ate [13.5]
(S)-2-butanol	D- and L- (or R and S): Ate [13.5];[b] Ser [14] and [2.8, 5.5, 8.3, 11, 14, 28];[c] Met [0.69, 2.1, 3.4], [3.4, 5.5, 7.6],[c] and [3.4, 5.5, 7.6];[d] Phe [1.4, 2.8, 4.1, 5.5] and [0.28, 0.55, 0.83, 1.1, 1.4]. Racemic mixtures of Tyr, Pen, Try, Thr, Phe, Ser [1.7, 3.4, 5.2, 6.9, 14];[e] Met [3.4, 5.2];[e] Ser, Ate, G [0.28, 0.55, 0.83, 1.1];[f] D- and L-valinol, racemic mixtures of valinol [0.75]; Phe, His, Arg, Lys [1.7, 3.4, 6.9]
tFMBA	Racemic mixtures of Ser, Thr, Met, Phe, Tyr, Try, Ate, valinol [0.28, 1.2, 1.7, 2.3]
(L)-ethyl lactate	D- and L- valinol [3.3, 6.6, 13, 26, 55, 110]
Methyl (S)-2-chloropropionate	Valinol (D- and L-) and Atenolol (R and S) [0.11]

[a] Buffer gas temperatures of 110, 140, 170 and 200°C were tested; [b] 4 experiments on two days; [c] Two experiments on two days; [d] at 138°C; [e] at 100, 150, 200, and 250°C, two experiments on different days; [f] analyte concentrations of 50, 250 and 1000 µM were tested. Several of these experiments included repetitions at different times. Arg: arginine, Ate: atenolol, G: glucose, His: histidine, Lys: lysine, Met: methionine, Pen: penicillamine, Phe: phenylalanine, Ser: serine, tFMBA: (R)-α-(trifluoromethyl) benzyl alcohol, Thr: threonine, Try: tryptophan, Tyr: tyrosine, Val: valine

Many solutions of racemic mixtures and individual enantiomers were analyzed by injecting seven chiral selectors into the buffer gas in 68 experiments (Table 1) to determine the possibility of enantiomer separation. The racemic mixtures could not be separated nor did the enantiomers show different drift times using different concentrations of chiral selectors (Figure 1) or buffer gas temperatures. Appendices 2 and 3 describe two experiments using different concentrations of chiral selectors or buffer gas temperatures, respectively, where the enantiomers produced different drift times, although not enough to separate a racemic mixture; these results could not be reproduced.

Table 1 summarizes the following experiments:

- (R)-1-phenyl ethanol was used as the chiral selector at 5.3 mmol m^{-3} for the analysis of individual 500-µM enantiomer solutions of asparagine, methionine, and phenylalanine at 150°C. In another experiment, these amino acids were tested at 2.1, 4.2, and 6.3 mmol m^{-3} (R)-1-phenyl ethanol under the same experimental conditions.
- (S)-1-phenyl ethanol was used as the chiral selector at 0.42 and 0.63 mmol m^{-3} for the analysis of individual 500-µM enantiomer solutions of phenylalanine and atenolol at 150°C. In another experiment, individual enantiomers of atenolol were tested at 5.3 mmol m^{-3} (S)-1-phenyl ethanol under the same experimental conditions.
- (R)-2-butanol was used as the chiral selector at 0.69 mmol m^{-3}; 4.8, 6.2, 7.6 and 14 mmol m^{-3}; 3.4, 5.5, 7.6 mmol m^{-3}; and 1.4, 2.8, 4.1, 5.5, 6.9, 8.3 mmol m^{-3} for the analysis of individual 500-µM solutions of methionine enantiomers at 150°C in four different experiments. In another experiment, the following 500-µM racemic mixtures were

analyzed under the same experimental conditions: atenolol with 13.5 mmol m^{-3} (R)-2-butanol, serine with 6.9 mmol m^{-3} (R)-2-butanol at 110, 140, 170 and 200°C, tyrosine with 6.1 mmol m^{-3} (R)-2-butanol, and valinol and valine, in four experiments on different days, with 6.8 mmol m^{-3} (R)-2-butanol.

- (S)-2-butanol was used as the chiral selector with the following individual enantiomers: 500-µM R and S-atenolol with 13.5 mmol m^{-3} (S)-2-butanol in 4 experiments during two days; 250-µM D- and L-serine with 2.8, 5.5, 8.3, 11, and 14 mmol m^{-3} (S)-2-butanol in two different experiments; 500-µM methionine at 0.69, 2.1, and 3.4 mmol m^{-3} (S)-2-butanol in one experiment, 3.4, 5.5, and 7.6 mmol m^{-3} (S)-2-butanol in two additional experiments on two days at 150 and 138°C; 500-µM D- and L-phenylalanine at 1.4, 2.8, 4.1, and 5.5 mmol m^{-3} (S)-2-butanol, and 0.28, 0.55, 0.83, 1.1, 1.4 mmol m^{-3} (S)-2-butanol in another experiment. The following racemic mixtures were analyzed: tyrosine, penicillamine, tryptophan, threonine, phenylalanine, and serine with 1.7, 3.4, 5.2, 6.9, 14 mmol m^{-3} (S)-2-butanol at 100, 150, 200, and 250°C, in two experiments on different days; methionine at 3.4 and 5.2 mmol m^{-3} (S)-2-butanol at 100, 150, 200, and 250°C, in two experiments on different days; 50-, 250- and 1000-µM serine, atenolol, and glucose at 0.28, 0.55, 0.83, and 1.1 mmol m^{-3} (S)-2-butanol with several repetitions at different times; D- and L-valinol at 10, 50, 250, and 943 µM and 250- and 943-µM racemic mixtures of valinol with 0.75 mmol m^{-3} (S)-2-butanol at 150 °C, and phenylalanine, histidine, arginine, and lysine with 1.7, 3.4, 6.9 mmol m^{-3} (S)-2-butanol.
- (R)-α-(trifluoromethyl) benzyl alcohol was used as the chiral selector at 0.3, 0.55, 1.1, 1.7, and 2.3 mmol m^{-3} for the analysis of 500-µM racemic mixtures of serine, threonine, methionine, phenylalanine, tyrosine, tryptophan, atenolol, and valinol at 150°C.
- Ethyl lactate was used as the chiral selector at 3.3, 6.6, 13, 26, 55, and 110 mmol m^{-3} for the analisis of 500-µM solutions of valinol enantiomers at 150°C.
- Methyl (S)-2-chloropropionate was used as the chiral selector at a 0.09 mmol m^{-3} for the análisis of 500-µM solutions of enantiomers of valinol and atenolol at 150°C.

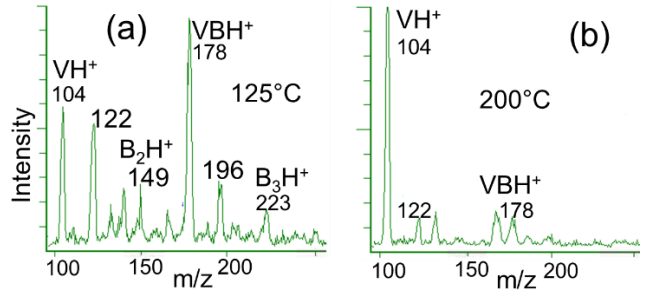

Figure 2. Extensive formation of clusters at low temperatures. (a) MS spectrum of valinol, V, at 125 °C and (b) at 200 °C. (S)-2-butanol, B, in the buffer gas: 0.28 mmol m^{-3}; valinol: 943 µM. A large VBH^+ peak (*m/z* 178) and dimer (B_2H^+, *m/z* 149) and trimer (B_3H^+, *m/z* 223) peaks of (S)-2-butanol are seen at 125°C (a). At 200 °C, only a small VBH^+ peak and a large VH^+ peak are observed because the B_2H^+ and B_3H^+ clusters disappeared, due to weak electrostatic interactions at high temperatures (b). The hydrated valinol ion, VH_3O^+, is observed at *m/z* 122.

The weak valinol:(S)-2-butanol interaction at high temperatures (Appendices 2 and 3) is consistent with the mass spectral data. Figure 2a shows a large valinol-(S)-2-butanol cluster

peak (*m/z* 178) and cluster peaks of (S)-2-butanol (at *m/z* 149 and 223) at low temperatures (125°C) but the high-temperature spectrum (200 °C, Figure 2b) only showed a small valinol-(S)-2-butanol peak together with a large peak of protonated valinol. Additionally, the drift times of valinol remained unchanged when increasing the chiral selector concentration at 200°C (Appendix 2) and the (S)-2-butanol dimer (*m/z* 149) and trimer (*m/z* 223) did not appear in Figure 2b.

3. Analyte concentration and enantiomer separation

The effect of valinol concentration was not important on the mobilities of its enantiomers when (S)-2-butanol was introduced into the buffer gas under the experimental conditions (Appendix 4). Five experiments injecting solutions of D- and L-valinol at concentrations of 10, 50, 250, and 943 µM and racemic mixtures of valinol at concentrations of 250 and 943 µM with 0.75 mmol m^{-3} of (S)-2-butanol in the buffer gas at 150 °C yielded negative results (Table 1).

4. Type of chiral selector and enantiomer separation

(R) and (S)-1-phenyl ethanol, (R) and (S)-2-butanol, (R)-tetrahydrofuran-2-carbonitrile (tHFCN), and (R)-α-(trifluoromethyl) benzyl alcohol were unsuccessfully tested as chiral selectors for racemic mixtures of the compounds listed in Table 1 in 62 diverse experiments under the specific conditions used.

5. Effect of other parameters on enantiomer separation

Buffer gas flow rates, ESI voltage, ESI solvent acidity, and proportions of D and L-enantiomers in the racemic mixture were varied to obtain enantiomer separations. We tested a 50-µM racemic mixture of valine with 6.8 mmol m^{-3} (R)-2-butanol in the buffer gas as the chiral selector at 175°C (unless other conditions are specified) by changing a single experimental condition to find better conditions for separation or to rule out racemization. No separation of the racemic mixtures was observed in these experiments:

1. **Buffer gas flow rates**. Different buffer gas flow rates (3.6, 1.8, 0.9, and 0.45 L min^{-1}) were used. These experiments were performed because low buffer gas flow rates increase the chiral selector concentration in the buffer gas and this could increase the possibility of enantiomer separation.
2. **ESI voltage**. The ESI voltage was varied between 15.6 and 13.9 kV to rule out racemization induced by high voltages at the ion source. Voltage differences of 3.5, 2.8, 2.4, 2.1, 1.9, and 1.8 kV were tested with respect to the target screen. The IMS signal was lost at a 1.8 kV difference due to absence of nebulization at those low voltages.
3. **ESI solvent acidity**. Acetic acid concentrations were tested at 5%, 1%, 0.1%, 0.03% and 0.01% in the ESI solution. The IMS signal was lost below 0.01% due to insufficient protonation of valine.
4. **Proportions of D and L-enantiomers in the racemic mixture.** D and L-enantiomers of valine were tested in 10:90, 30:70, 70:30, and 90:10 (v/v) ratios. The reason for these experiments was that the racemic mixture, in a few experiments (Appendices 1-4), yielded a drift time similar to that of D-valine. Therefore, racemization was speculated

when they were mixed or upon interacting with the hot metallic surface of the gas heater. Analyses of these mixtures might show a shift from the drift time of D-valine to that of L-valine when the concentration of L-valine increased in the mixture if this conversion was occurring. However, that shift was not observed.

6. Theoretical considerations

Several possible interactions between chiral 2-butanol and the enantiomers of atenolol, serine, and valinol cations were studied. These species were selected because they have the highest and lowest molecular weights and the effects of adduction of 2-butanol on their ion mobilities are the smallest and largest, respectively; this is important for the comparisons we will make. In amino acids, the most energetically favorable hydrogen bond is produced by the interaction of the hydroxyl group of 2-butanol with the protonated amino group of the analyte but the bonding could also occur via the carboxylic group; Figure S5 shows the phenylalanine:2-butanol interaction. Figures of the isolated chiral cations and complexes are shown in the Supporting Information (Figures S6-S8). In all the complexes between 2-butanol and atenolol, serine, and valinol, a hydrogen bond was formed between the protonated amino group of the chiral cation and the OH group of 2-butanol. In atenolol complexes, an additional hydrogen bond was formed between the OH group of 2-butanol and the oxygen atom of the amide group of atenolol.

The formation energies of the complexes formed between (S)-2-butanol and the R- or S-enantiomers chiral cations (Table 2) obtained with the two functionals and basis sets were very similar and exothermic. However, the large enthalpy was largely offset by a loss of entropy, which was largest for atenolol, which also had the smallest binding enthalpy, making the complex formation endergonic in this case. The formations of serine and valinol complexes were all exergonic.

Table 2. Electronic complex formation energies (ΔE, electronic energy differences without zero-point vibrational energies), Gibbs free energies (ΔG), enthalpies (ΔH), and entropies (reported as $T\Delta S$) of the complex formation reactions studied (kJ/mol).

Complex	**B97-3c**					**ωB97X-V/def2-QZVP//B97-3c**	
	ΔE	***ΔG***	$\overline{\Delta G}$	***ΔH***	***TΔS***	***ΔE***	***ΔG***
R-A · S-B	-69.0	11.2	11.8	-62.2	-73.4	-71.2	9.0
S-A · S-B	-68.9	12.4		-61.4	-73.8	-71.0	10.3
R-Ser · S-B	-94.3	-22.1	-22.6	-87.5	-65.3	-92.7	-20.5
S-Ser · S-B	-95.2	-23.2		-88.4	-65.2	-94.9	-22.9
R-V · S-B	-86.5	-13.4	-12.8	-79.5	-66.1	-85.1	-12.0
S-V · S-B	-84.6	-12.3		-77.9	-65.6	-82.3	-10.0
Complex	**ΔΔG***					**ΔΔG****	
Atenolol	1.3					1.5	
Serine	-1.0					-2.4	
Valinol	-1.4					-2.2	

A: atenolol; S-B: (S)-2-butanol; Ser: serine; V: valinol. $\overline{\Delta G}$: average Gibbs free energies of the complex formation reactions. $\Delta\Delta G$: differences of the complex stabilities of the R- and S-enantiomers of the same cation with (S)-2-butanol calculated directly from the complexes (not as differences of ΔG values from the table) evaluated with

B97-3c (*) or ωB97X-V/def2-QZVP//B97-3c (**). These $\Delta\Delta G$ values differed slightly from those calculated from ΔG because the free energies of the isolated R- and S-enantiomers of the chiral cation were slightly different in our calculations.

An important aspect was the relative stability of the complexes between chiral butanol and the R- and S-enantiomers of the chiral analytes. This stability governs the drift time: the more stable the complex, the longer the species drift as the large complex, thus experiencing a more significant number of collisions with nitrogen drift gas than less stable species increasing its drift time. The greater the difference in relative stability of the complexes between chiral butanol and the R- and S-enantiomers, $\Delta\Delta G$, the greater the difference in their drift times and the more plausible the enantiomer separation will be. The values of $\Delta\Delta G$ are generally very small (Table 2), both in terms of energies or free energies, with differences of ~1-3 kJ/mol.

7. Critical review of previous reports on enantiomer separation

In 2006, Dwivedi *et al.* reported the separation of racemic mixtures after the introduction of (S)-2-butanol in the buffer gas of a drift-time ion mobility spectrometer,[12] the same laboratory, instrument, conditions, and reagents used in our investigation. Those results are inconsistent because (Figure 3):

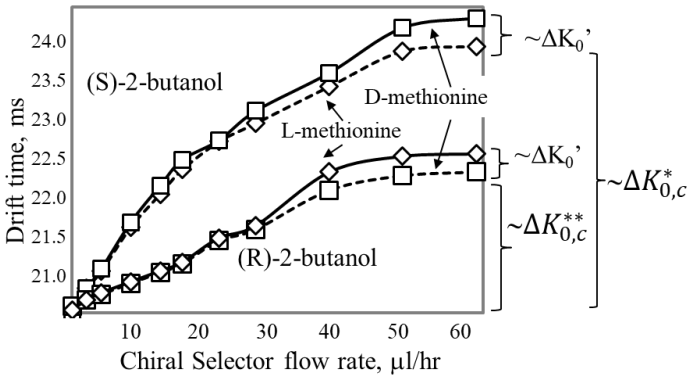

Figure 3. Drift time shifts of methionine enantiomers in the buffer gas after introduction of (S)-2-butanol vapor (built from data in Table 2 in reference 12).[12] $\sim\Delta K_0'$ and $\sim\Delta K_{0,c}$ mean that these drift times ranges are proportional to $\Delta K_0'$, percentage mobility difference between enantiomers of the same cation in (S)-2-butanol-doped buffer gas (mobility shift due to chiral differences), and to $\Delta K_{0,c}$, percentage change in K_0 when the butanol flow rate was varied (the achiral mobility shift).

a) **The curve of (R)-2-butanol must overlap that of (S)-2-butanol** because the adducts L-methionine/(R)-2-butanol and L-methionine/(S)-2-butanol are the specular images of D-methionine/(S)-2-butanol and D-methionine/(R)-2-butanol, respectively, and, therefore, must drift the same time because they have the same size and energetics. However, they were very different.

b) **The separation between the curves** of L-methionine/(R)-2-butanol and D-methionine/(R)-2-butanol (lower curves), and that of D-methionine/(S)-2-butanol and L-methionine/(S)-2-butanol (upper curves) must be identical by the same reasoning used in literal a. However, they were different.

c) **The separation between atenolol enantiomers, ΔK_0', was too large**, 1.7% (Table 3, bold), compared with those of the other racemic mixtures. It was greater than those of smaller molecules such as tryptophan (1.6%), methionine (0.8%), glucose (1.6%), penicillamine (1.4%), and valinol (1.2%) (Table S3). With a larger size, atenolol should have given a smaller ΔK_0' than those of the species mentioned above, because a large size decreases the effect of buffer additives on the mobilities.[20,30,31]Atenolol is a large compound that has shown only a small absolute mobility shift of 0.7% with 2-butanol in the buffer gas for strong non-chiral interactions.[32] For this reason, it is not clear how a large 1.7% mobility shift, ΔK_0', can be obtained for a weak chiral interaction especially because its non-chiral interaction, stronger than a chiral interaction, for the (S)-atenolol enantiomer ($\Delta K_{0,c}$) yielded a 0% mobility shift, it did not shift, in close agreement with our non-chiral experiments.[20,30-32] As a confirmation of this observation, the atenolol complex formation was endergonic with an average formation ΔG of 11.8 kJ/mol (Table 2), so its enantiomers should not have shown any mobility shift with the introduction of 2-butanol into the buffer gas.

d) **The separation between the D- and L-enantiomers of the same species, ΔK_0', was too large compared to $\Delta K_{0,c}$** (Table 3, Figure S9). The $\Delta\Delta G$ values calculated from the species in reference 12 were small (Table 2) as expected from chiral interactions: only 1.3 kJ/mol (0.31 kcal/mol), -1.0 kJ/mol (0.24 kcal/mol), and 1.4 kJ/mol (0.33 kcal/mol) for atenolol, serine and valinol, respectively,[12] too small to account for the relatively large enantiomer separations reported. To visualize this, we have to compare the ratio of ΔK_0' and $\Delta K_{0,c}$ with respect to $\Delta\Delta G$ and ΔG_D, respectively (Table 3, last two columns). The D-enantiomer shift, the smallest shift, is considered the mobility shift due to achiral interactions. $\frac{\Delta K_{0,c}}{\Delta G_D}$ and $\frac{\Delta K_0'}{\overline{\Delta\Delta G}}$ are a measure of mobility shifts caused by the complex bonding strength (mobility shifts due to achiral interactions) and chiral interaction, respectively. For valinol and serine, taken as examples, $\frac{\Delta K_{0,c}}{\Delta G_D} < \frac{\Delta K_0'}{\overline{\Delta\Delta G}}$. This means that the relative mobility shifts produced by chiral interactions in these complexes were greater than those produced by non-chiral interactions, contrary to expectations because chiral interactions are weaker than the strong non-chiral interaction, specially with the formal charge on the cation. A graphical explanation of this reasoning appears in Figure S9. The strong non-chiral interactions cancel out chiral interactions because these requiere a given spatial relationship between the cluster components that is broken by the strong formal charge. Performing these calculations using Gaussian, the molecule:ion ensemble rearranged at the same given position due to strong interaction of the formal charge. Therefore, $\Delta\Delta G$ could not be initially calculated with this program.

Table 3. ΔK_0' and $\Delta K_{0,c}$ for data from reference 12.[12] Butanol flow rate in the buffer gas was varied from 0.0 to 65 µL/hr. The complete data set of these experiments is shown in Table S3. K_0 units in $cm^2v^{-1}s^{-1}$.

Species	K_0 value in N_2	Mean drift time in N_2, ms	K_0 in (S)-2-butanol		ΔK_0' (%)	$\Delta K_{0,c}$ (%) D-ee	$\overline{\Delta\Delta G}$	ΔG_D	$\frac{\Delta K_{0,c}}{\Delta G_D}$	$\frac{\Delta K_0'}{\overline{\Delta\Delta G}}$
			D-ee	L-ee						
Atenolol	1.18	-	1.18[&]	1.16*	**1.7**	-1.7*	[#]	[#]	[#]	[#]
Valinol	1.74	16.735	1.60	1.62	*-1.2*	-8.0	-1.8	-13.4	0.60[¥]	0.69
Serine	1.73	16.825	1.55	1.52	-1.9	-10.4	-1.7	-22.1	0.47[¥]	1.14

ee: Enantiomer. [&]R-atenolol; *S-atenolol. ΔK_0': percentage mobility difference between enantiomers of the same cation in (S)-2-butanol-doped buffer gas. $\Delta K_{0,c}$: percentage change in K_0 when the butanol flow rate was varied. $\overline{\Delta\Delta G}$: average of the complex stabilitiy differences of the R- and S-enantiomers of the same cation with (S)-2-butanol obtained with both functionals in Table 2. ΔG_D: Gibbs free energy of the complex formation reaction of the R-enantiomer in Table 2. [#] For atenolol, these values would be meaningless because its formation was endergonic. The 1.2 value for ΔK_0' of valinol (in italics) was calculated as [(1.60-1.62)/1.62]x100; -8.0 for $\Delta K_{0,c}$ of D-valinol as [(1.60-1.74)/1.74]x100; 1.8 as the mean of $\Delta\Delta G$ values -1.4 and -2.2 in Table 2; 0.60 as -8.0/-13.4; and 0.69 as -1.2/-1.8; $\frac{\Delta K_{0,c}}{\Delta G_D}$ was calculated using $\Delta K_{0,c}$ of the D-enantiomers,[¥] instead $\Delta K_{0,c}$ average, to shorten this table; Table S4 shows these calculations using average $\Delta K_{0,c}$. This did not change our results or conclusions. A graphical explanation of this table appears in Figure S9.

e) The temperature of the drift region, desolvation region, and drift gas was maintained at 200 °C. At this relatively high temperature, there is a smaller effect of 2-butanol on the drift times of the analytes, Appendix 2 and literature reports,[30,31] because at high temperatures the bonds are easier to break and the change in drift time should be smaller given that the ions travel most of the time as the non-complexed species. This means that the differences described in literals c and d would be greater because our experiments were performed mostly at 150°C. Furthermore, Zehnacker (2014) concluded that the studies of supplementary interactions accounting for chiral recognition in spectroscopy and photophysics of complexes of chiral species should be performed at low temperatures because these interactions would be obscured at room temperature.[19] For this reason, IMS enantiomer separations at high temperatures would be even more difficult.

f) The mass-mobility correlation was poor. The correlation between analyte masses and their ion mobility has been recognized long ago.[33] However, correlation coefficients of only 0.24 and 0.45 were obtained from reference 12 between the mass and ΔK_0' and $\Delta K_{0,c}$, respectively (Table S3). Using similar compounds, we obtained a correlation coefficient of 0.74 for the mass-K_0 correlation [30] and 0.76 for the mass-$\Delta K_{0,c}$ correlation [34] using 2-butanol as a shift reagent, the chiral selector of reference 12.[12] Correlation between mass and ΔK_0' should also be obtained because as the chiral compound mass increases, ΔK_0' should decrease since large compounds show small mobility shifts. Those small coefficients above may indicate that the data supporting the enantiomer separations reported may not be reliable.

The separation of fluoxetine enantiomers claimed by Karas [13] is only discussed in Appendix 5 as it is in a non-peer-reviewed document. Recommendations for potential enantiomer separations by IMS are given in Appendix 6.

CONCLUSIONS

In contrast to a previous study, [12] no enantiomer separation was obtained when the separation of racemic mixtures was tested by introducing chiral selectors into the buffer gas of a drift tube ion mobility-mass spectrometer. There have been no other reported separations after sixteen years of the only published experiment that claimed enantiomer separation by drift tube IMS. [12] Additionally, several attempts to reproduce those experiments, most of them using the same reagents, instrument, personnel, and conditions of the original study, have yielded negative results.

The lack of separation of the racemic mixtures might have occurred because we did not reproduce the precise conditions used in the previous study.[12] Reference 12 reported enantiomer separations on different days for twelve chiral compounds. Because of this number, these experiments had to be run on several different days, most probably under different conditions of temperature, pressure, and more. Therefore, experimental conditions should not be so critical that we could not find them in the thousands of analyses performed. Moreover, we had unsuccessful assistance from the former team to reproduce their previous results, so this assumption should be discarded. An improper preparation of the racemic mixture cannot be argued because these mixtures were prepared weekly during 18 months.

The lack of separation of the racemic mixtures was not produced by racemization because in symmetric environments as the ESI solution both enantiomers have the same stability. Acid racemization has been widely demonstrated in amino acids [35] and could happen due to ESI solution acidic conditions used as a solvent. Bada found that the racemization reactions rate constants were about 10^{-11} at 25 °C and pH 2, similar to that of the ESI solvent used in this study.[36] These speeds are negligible although our experiments were at 150°C, in the gas phase, and under an electric field of 432 V. Nevertheless, racemization of our reagents would require the breaking of C-H, C-C, C-N, or C-O bonds or the presence of enzymes.[35] Another explanation is that one of the enantiomers has a stronger proton affinity and keeps all the available protons but, again, protons are symmetric and enantiomers must have the same proton affinity. A plausible explanation for the negative results is that the IMS resolving power was not enough to show the separation of enantiomers in racemic mixtures but statistically different drift times should have been obtained for individual enantiomers consistently. Our racemic mixtures rarely showed even shoulders on the peaks of the spectra.

Finally, energy calculations of the chiral selector–ion interactions showed that these separations are unlikely. Future work must focus on understanding the chemistry underlying the singular behavior of the racemic mixture in a drift tube in the presence of a chiral selector and finding enantiomers that yield larger complex stability differences that can produce enough separation using a high resolution IMS spectrometer.

ACKNOWLEDGEMENTS

The corresponding author thanks the kind help of Herbert Hill and Bill Siems in WSU for the discussion of Figure 3, central to this paper. This article is dedicated to them. Financial support

was provided by a Fulbright scholarship, Universidad de Cartagena, Washington State University, and Herbert Hill lab.

The authors declare that they have no known competing financial interests or personal relationships that could have appeared to influence the work reported in this paper.

Doerr did the theoretical studies and Fernandez the experiments.

SUPPORTING INFORMATION

Fig. S1. Photograph of ESI-IMS-MS spectrometer.
Fig. S2. Chiral analytes and chiral selectors for enantiomer separation experiments
Fig. S3. IMS spectra of racemic mixtures or enantiomers with (S)-2-butanol in the buffer gas.
Fig. S4. L-valinol IMS spectrum showing the resolution of the instrument.
Fig. S5. Drawing of phenylalanine:2-butanol interaction.
Fig. S6-S8. Structures of isolated chiral cations and their complexes with 2-butanol.
Fig. S9. Graphical explanation of Table 3.
Fig. S10. Mass spectra showing an extensive formation of clusters at high (S)-2-butanol concentrations.
Table S1. Review of seven studies cited by Nagy et al.[6] about enantiomer separations.
Table S2. Resolving power of the IMS instrument for selected peaks of phenylalanine.
Table S3. $\Delta K0'$ and $\Delta K0,c$: values for experiments from Table 1 in reference 12.
Table S4. Complete version of Table 3
Table S5. Chiral experiments with D and L phenylalanine.
Table S6. Drift times of valine enantiomers over an 8-hr period using (S)-2-butanol chiral selector
Table S7. Effect of chiral selector concentration on the mobilities of valinol enantiomers at 125 and 200°C
APPENDIX 1. Stability of the mobilities of valine enantiomers with time
APPENDIX 2. Chiral selector concentration and enantiomer separation
APPENDIX 3. Buffer gas temperature and separation of valinol enantiomers
APPENDIX 4. Analyte concentration and enantiomer separation
APPENDIX 5. Claimed separation of fluoxetine enantiomers
APPENDIX 6. Recommendations for potential enantiomer separations by IMS

REFERENCES

1. W.H. Pirkle, T.C. Pochapsky. Considerations of chiral recognition relevant to the liquid chromatography separation of enantiomers. *Chem. Rev.* **1989,** *89*, 347.

2. Schalley, C. A.; Hoernschemeyer, J.; Li, X.; Silva, G.; Weis, P. Distinguishing the topology of macrocyclic compounds and catenanes *Int. J. Mass Spectrom.* **2003**, *228,* 2-3, 373-388.

3. Davankov, V. A. (1997). The nature of chiral recognition: Is it a three-point interaction?. *Chirality*, *9*(2), 99-102.

4. Li, Z., Hu, C., Liu, Y., Li, Q., Fu, Y., & Chen, Z. (2021). Facile preparation of ethanediamine-β-cyclodextrin modified capillary column for electrochromatographic enantioseparation of Dansyl amino acids. *Journal of Chromatography A*, 462082.

5. J. Diana Zhang, K.M. Mohibul Kabir, W. Alexander Donald, Chapter Three - Ion-Mobility Mass Spectrometry for Chiral Analysis of Small Molecules, Editor(s): W. Alexander Donald, James S. Prell, Comprehensive Analytical Chemistry, Elsevier, Volume 83, 2019, 51-81

6. Nagy, G., Chouinard, C. D., Attah, I. K., Webb, I. K., Garimella, S. V., Ibrahim, Y. M., ... & Smith, R. D. (2018). Distinguishing enantiomeric amino acids with chiral cyclodextrin adducts and structures for lossless ion manipulations. Electrophoresis, 39(24), 3148-3155.

7. Sawada, M. (1997). Chiral recognition detected by fast atom bombardment mass spectrometry. *Mass spectrometry reviews*, *16*(2), 73-90.

8. Tao, W. A., & Cooks, R. G. (2003). Peer reviewed: chiral analysis by MS. *Analytical chemistry*, *75*, 25-A.

9. Wu, Q., Wang, J. Y., Han, D. Q., & Yao, Z. P. (2020). Recent advances in differentiation of isomers by ion mobility mass spectrometry. *TrAC Trends in Analytical Chemistry*, *124*, 115801.

10. K. Kulyk, O. Rebrov, M. Ryding, R.D. Thomas, E. Uggerud, M. Larsson. Low-Energy Collisions of Protonated Enantiopure Amino Acids with Chiral Target Gases. *J. Am. Chem. Soc. Mass Spectrom.* **2017,** 28, 2686.

11. Rister, A. L., & Dodds, E. D. (2020). Steroid analysis by ion mobility spectrometry. *Steroids*, *153*, 108531.

12. Dwivedi, P.; Wu, C.; Matz, L. M.; Clowers, B. H.; Siems, W. F.; Hill, H. H. Jr. Gas-phase chiral separations by ion mobility spectrometry. *Anal. Chem.* **2006**, *78*, 24, 8200-8206.

13. M. Karas. Separation of components of an analysis sample in an ion mobility spectrometer using a supply of selectively interactive gaseous particles. U.S. Patent No. 7015462B2. 21 Mar. **2006**.

14. Roscioli, K. M. (2012). Selective ionization and separation in ion mobility spectrometry. Ph.D. Thesis. DOI: 10.6084/m9.figshare.14697012

15. Pérez-Míguez, R. et al. (2019). Chiral discrimination of DL-amino acids by trapped ion mobility spectrometry after derivatization with (+)-1-(9-fluorenyl) ethyl chloroformate. *Analytical chemistry*, *91*(5), 3277-3285.

16. K. Kulyk *et al.* High-energy collisions of protonated enantiopure amino acids with a chiral target gas. *Int. J. Mass Spectrom.* **2015**, *388*, 59.

17. O. Rebrov, K. Kulyk, M. Ryding, R. Thomas, E. Uggerud, M. Larsson. Chirally sensitive collision induced dissociation of proton-bound diastereomeric complexes of tryptophan and 2-butanol. *Chirality*. **2017,** *29*, 115.

18. O. Rebrov; M. Poline; M. Mauritz; R. Thomas; E. Uggerud; M. Larsson. Non-covalently Bonded Diastereomeric Adducts of Amino Acids and (S)-1-Phenylethanol in Low-energy Dissociative Collisions. Mol. Phys. 2020, 118(4), 1615145.

19. Zehnacker, A. (2014). Chirality effects in gas-phase spectroscopy and photophysics of molecular and ionic complexes: contribution of low and room temperature studies. Int. Rev. Phys. Chem. 33(2), 151-207.

20. Fernandez-Maestre R. Buffer gas additives (modifiers/shift reagents) in ion mobility spectrometry: Applications, predictions of mobility shifts, and influence of interaction energy and structure. J Mass Spectrom. 2018 53(7) 598-613.

21. Wu, C., Siems, W. F., Asbury, G. R., & Hill, H. H. (1998). Electrospray ionization high-resolution ion mobility spectrometry− mass spectrometry. Anal. Chem. 70, 4929-4938.

22. Pracht, P., Bohle, F. & Grimme, S. Automated exploration of the low-energy chemical space with fast quantum chemical methods. *Phys. Chem. Chem. Phys.* (2020) doi:10.1039/C9CP06869D.

23. Bannwarth, C., Ehlert, S. & Grimme, S. GFN2-xTB—An Accurate and Broadly Parametrized Self-Consistent Tight-Binding Quantum Chemical Method with Multipole Electrostatics and Density-Dependent Dispersion Contributions. *J. Chem. Theory Comput.* **15**, 1652–1671 (2019).

24. Brandenburg, J. G., Bannwarth, C., Hansen, A. & Grimme, S. B97-3c: A revised low-cost variant of the B97-D density functional method. *J. Chem. Phys.* **148**, 064104 (2018).

25. Bell, E. W. & Zhang, Y. DockRMSD: an open-source tool for atom mapping and RMSD calculation of symmetric molecules through graph isomorphism. *J Cheminform* **11**, 40 (2019).

26. Mardirossian, N. & Head-Gordon, M. ωB97X-V: A 10-parameter, range-separated hybrid, generalized gradient approximation density functional with nonlocal correlation, designed by a survival-of-the-fittest strategy. *Phys. Chem. Chem. Phys.* **16**, 9904–9924 (2014).

27. Weigend, F. & Ahlrichs, R. Balanced basis sets of split valence, triple zeta valence and quadruple zeta valence quality for H to Rn: Design and assessment of accuracy. *Phys. Chem. Chem. Phys.* **7**, 3297–3305 (2005).

28. Neese, F. The ORCA program system. *WIREs Comput. Mol. Sci.* **2**, 73–78 (2012).

29. Neese, F. Software update: the ORCA program system, version 4.0. *WIREs Comput. Mol. Sci.* **8**, e1327 (2018).

30. Fernandez-Maestre R, Wu C, Hill HH. Using a Buffer Gas Modifier to Change Separation Selectivity in Ion Mobility Spectrometry, Int J Mass Spectrom 2010, 298, 2-9.

31. Fernandez-Maestre R, Wu C, Hill HH. Buffer gas modifiers effect resolution in ion mobility spectrometry through selective ion-molecule clustering reactions. Rapid Commun Mass Spectrom 2012, 26, 19, 2211–2223.

32. Fernandez-Maestre, R.; Harden, C.S.; Ewing, R.G.; Crawford, C.L.; Hill Jr., H.H. Chemical Standards in Ion Mobility Spectrometry. Analyst 2010, 135, 1433-1442.

33. Karasek, F. W., & Kane, D. M. (1972). Plasma chromatography of the n-alkyl alcohols. *J. Chrom. Sci. 10*, 673-677.

34. Fernandez-Maestre,R.; Tabrizchi, M. & Meza-Morelos, D. Ion-shift reagent binding energy and the shift-mass correlation in ion mobility spectrometry. Sent to J Mass Spectrom 13-12-2021. DOI: 10.26434/chemrxiv-2022-4cn0f

35. Kreil, G. (1994). Conversion of L- to D-amino acids: a posttranslational reaction. *Science*. *266*, 996-998. DOI: 10.1126/science.7973683

36. Bada, J. L. (1972). Kinetics of racemization of amino acids as a function of pH. *J. Am. Chem. Soc. 94*, 1371-1373.

On the Separation of Enantiomers by Drift Tube Ion Mobility Spectrometry

Roberto Fernández-Maestre,[1,2] *and Markus Doerr* [3]
[1] Departamento de Quimica, Campus de San Pablo, Universidad de Cartagena, Cartagena, Colombia.
[2] National Research Nuclear University MEPhI (Moscow Engineering Physics Institute), Kashirskoe sh. 31, Moscow, 115409, Russia. *rfernandezm@unicartagena.edu.co
[3] Universidad Industrial de Santander, Cra 27 Calle 9, Bucaramanga, Colombia. mhodoerr@uis.edu.co

Supporting Information

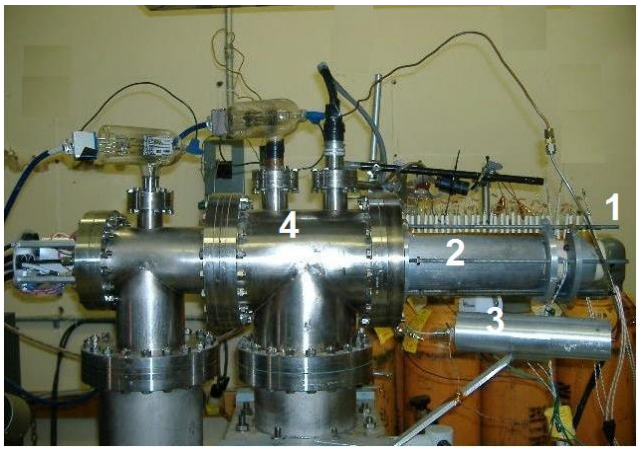

Figure S1. Photograph of the electrospray ionization-atmospheric pressure ion mobility-mass spectrometer. 1. Desolvation region 2. Drift region 3. Buffer gas heater 4. Mass spectrometer

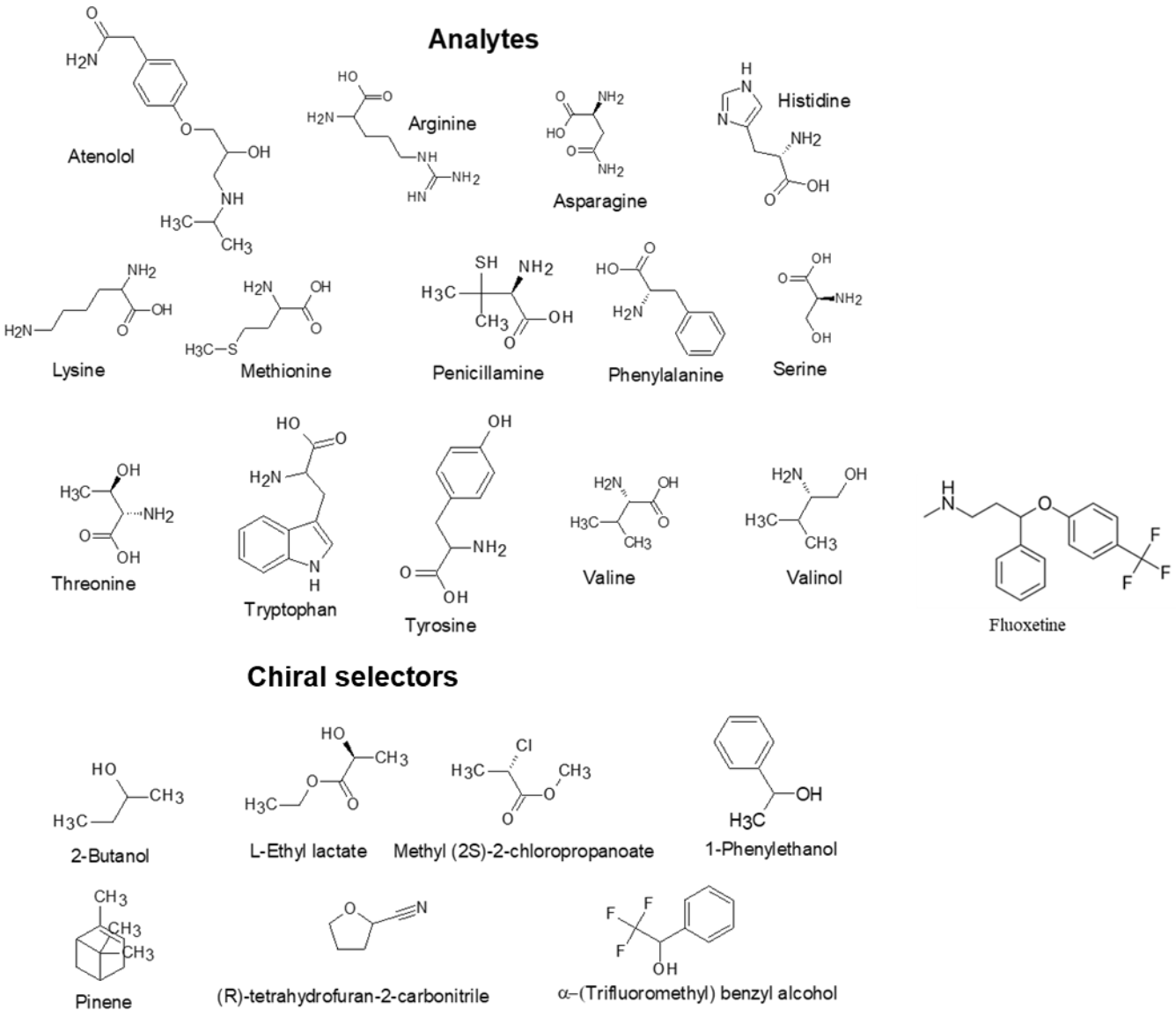

Figure S2. Chiral analytes and chiral selectors for enantiomer separation experiments

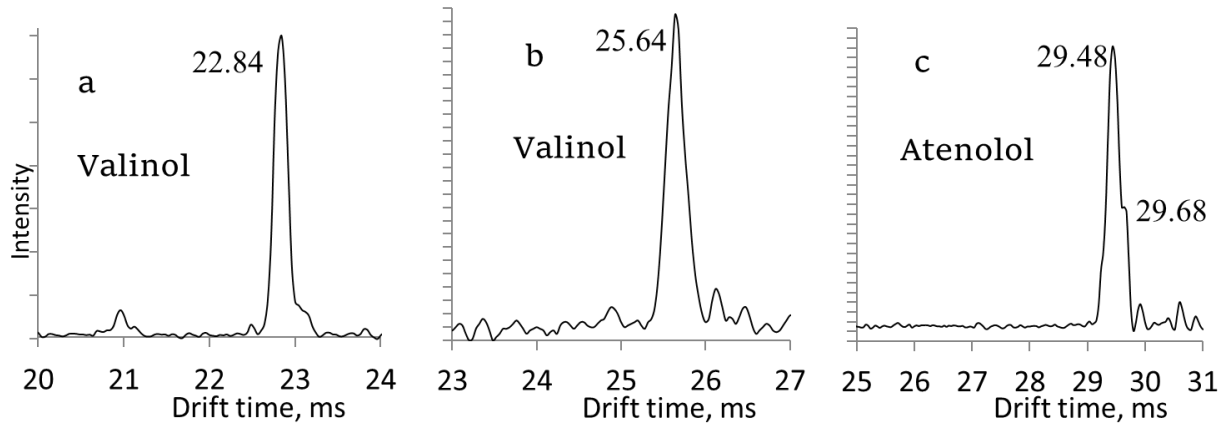

Figure S3. IMS spectra of racemic mixtures of 943-µM valinol at (S)-2-butanol flow rates of 45 µL/hr (a), 5 µL/hr (b), and (c) 100-µM atenolol at a (S)-2-butanol flow rate of 50 µL/hr in the buffer gas. Temperature was 150°C. No enantiomer separation is evident in these experiments.

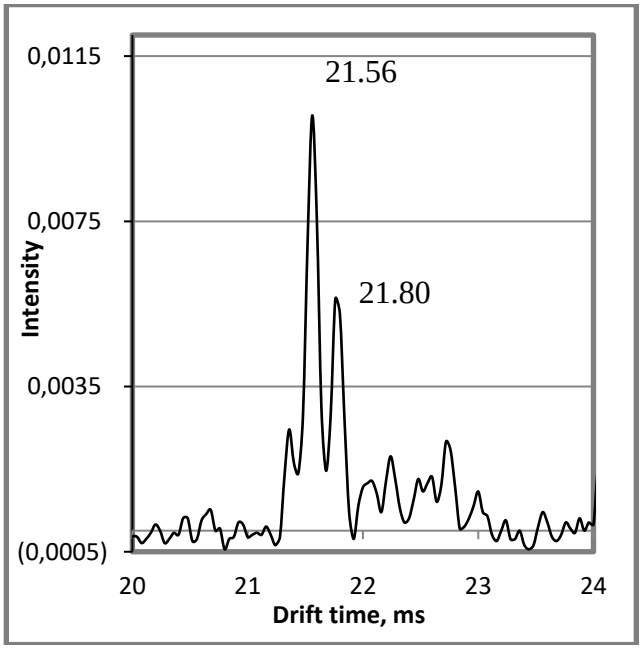

Figure S4. L-valinol IMS spectrum showing the resolution of the instrument and its capability to distinguish peaks separated by 0.24 ms or less. The peaks are separated by 0.24 ms and partially resolved.

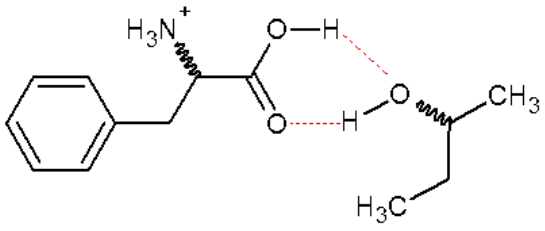

Interaction with the carboxylic group

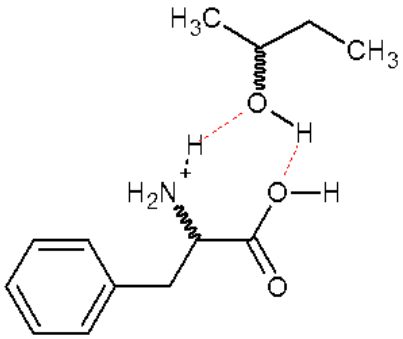

Interaction with the amine group

Figure S5. Phenylalanine:2-butanol interaction

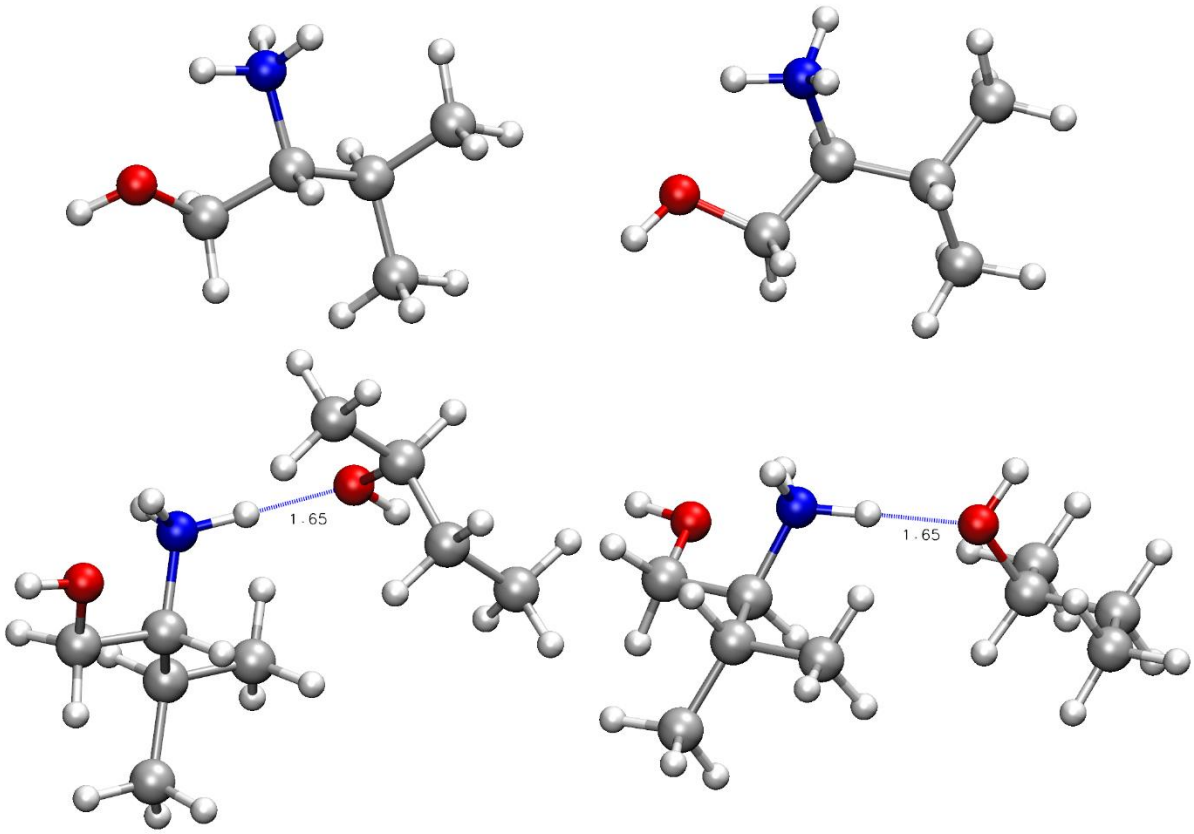

Figure S6. Isolated chiral valinol cations (above) and their complexes with 2-butanol (below). All figures were created with VMD.

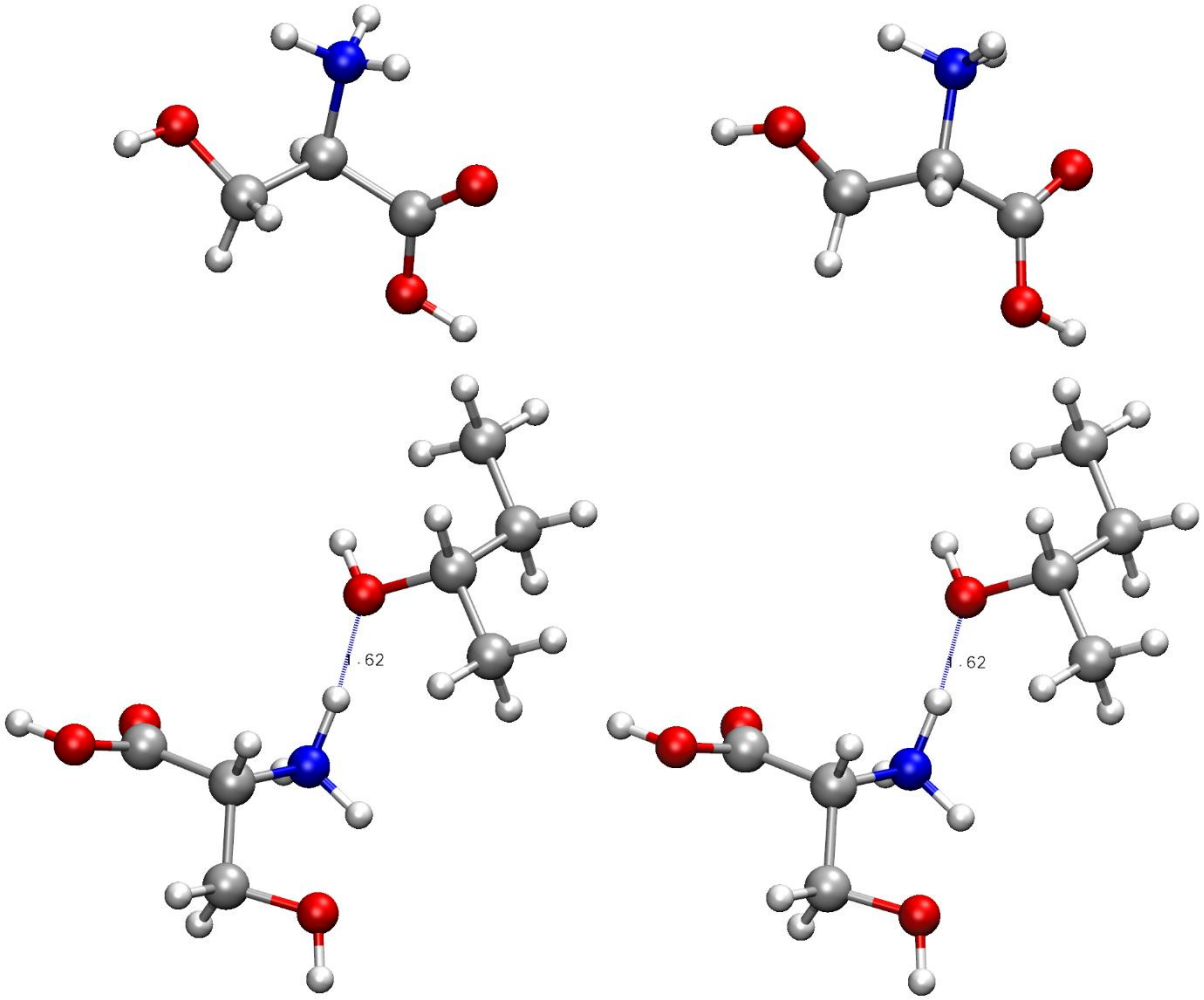

Figure S7. Isolated chiral serine cations (above) and their complexes with 2-butanol (below). All figures were created with VMD.

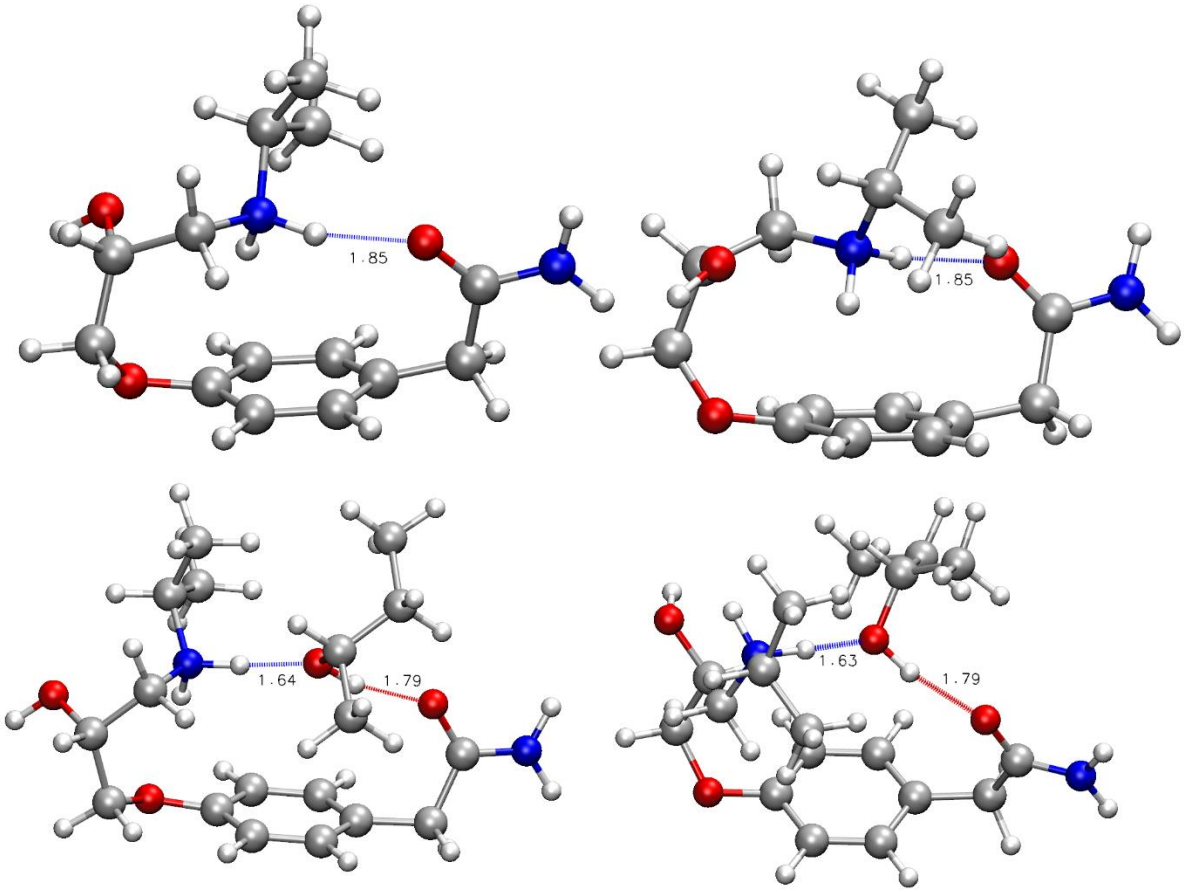

Figure S8. Isolated chiral atenolol cations (above) and their complexes with 2-butanol (below). All figures were created with VMD.

Figure S9. Graphical explanation of Table 3. Mobility shifts of valinol enantiomers after the introduction of (S)-2-butanol in the buffer gas (Mobilities and flow rate data from reference 12)[12].

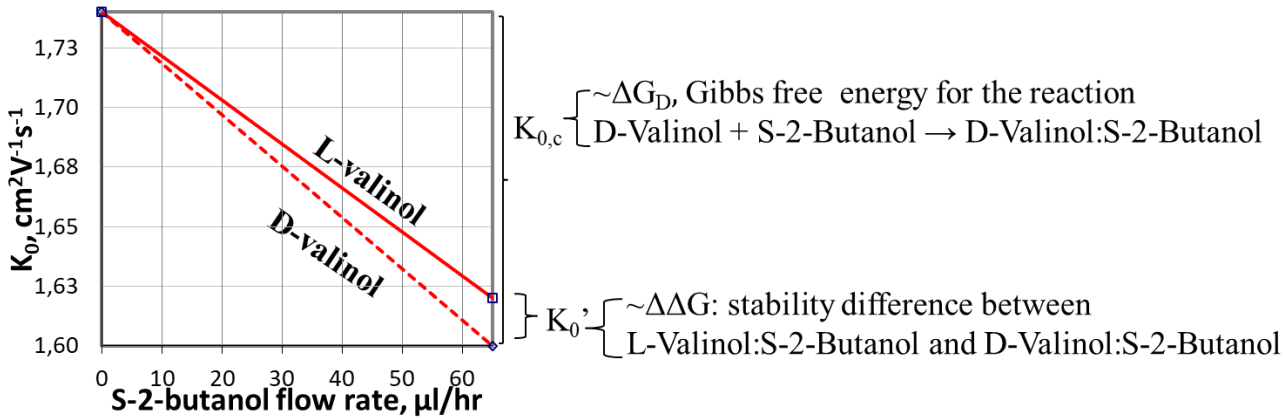

$K_{0,c}$ is the mobility shift when 2-butanol was injected in the buffer gas. K_0' is the separation between the D and L enantiomers, in mobility units. This is produced by the preferential size increase of one of the enantiomers over the other after clustering with 2-butanol and the concomitat increase in collisions against the buffer gas. The energetics determine the lifespan of these clusters. Therefore, ΔG_D, the Gibbs free energies for the formation reactions of the R-enantiomer in Table 2, determines $\Delta K_{0,c}$ (proportional to $K_{0,c}$). $\Delta\Delta G$, the difference of the stabilities between these two clusters, determines ΔK_0' (proportional to K_0'). Consequently, the values of $\Delta\Delta G$ and ΔG_D must be proportional to ΔK_0' and $\Delta K_{0,c}$, respectively; thus, $\frac{\Delta K_0'}{\Delta\Delta G}$ and $\frac{\Delta K_{0,c}}{\Delta G_D}$ must be similar because if the numerator increases (for example, when changing the species), the denominator also increases. Because $\frac{\Delta K_0'}{\Delta\Delta G} > \frac{\Delta K_{0,c}}{\Delta G_D}$, ΔK_0' and $\Delta\Delta G$ must be relatively large and small, respectively. This would indicate that the mobility shifts produced by the chiral interactions in the D-valinol:(S)-2-butanol complex would be relatively larger than those produced by non-chiral interactions. These results would be contrary to expectations because chiral interactions in these complexes are weaker than their strong non-chiral interactions, including the interaction with the formal charge on the cation.

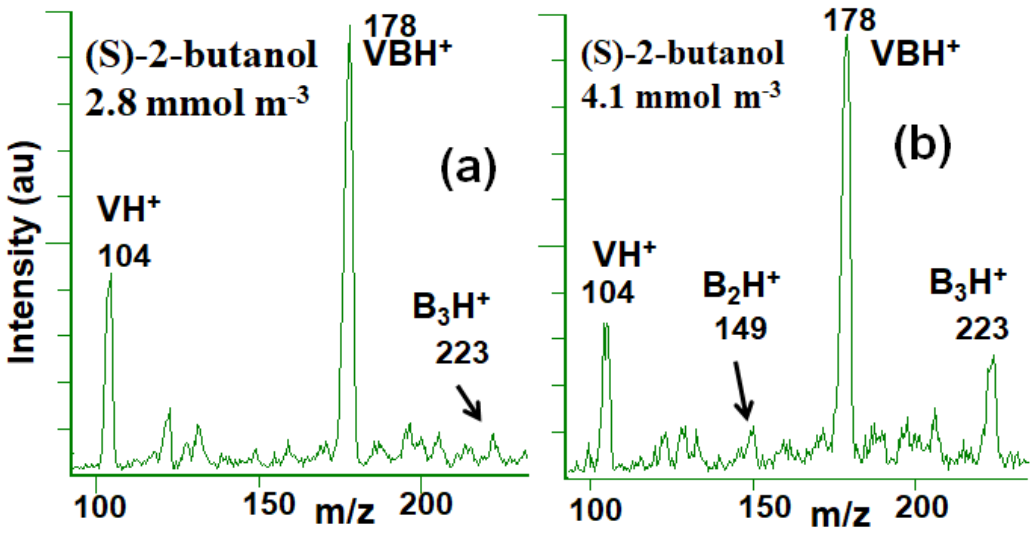

Figure S10. Increasing formation of clusters at high (S)-2-butanol concentrations. MS spectra of a 943-µM solution of D-valinol (V) at 150 °C when the concentration of (S)-2-butanol (B) in the buffer gas increased from (a) 2.8 mmol m^{-3} to (b) 4.1 mmol m^{-3}. Other experimental conditions were those of Appendix 1. When the (S)-2-butanol concentration increased, the intensity of VH^+ decreased with respect to VBH^+ because this cluster increased, as expected if the cluster was formed from protonated valinol, VH^+. The formation of large valinol-(S)-2-butanol clusters (*m/z* 178) explained the mobility reduction of valinol and serine from 1.62 to 1.60 and 1.55 to 1.73 $cm^2\ V^{-1}s^{-1}$, respectively (Table 3) when (S)-2-butanol was introduced into the buffer gas. This figure also illustrates the expected increase in intensity of the peaks of the dimer (B_2H^+, *m/z* 149) and trimer (B_3H^+, *m/z* 223) of (S)-2-butanol when the chiral selector concentration increased.

Table S1. Review of seven studies cited by Nagy et al.[6] about enantiomer separations. Any of these studies performed enantiomer separation by injecting only a chiral selector. Most of the studies separated enantiomers by forming chiral non-covalent diastereomeric complexes with other chiral molecules using transition metal cations.

Analytes	Method	Reference in Nagy paper
l-glucose, d-glucose, l-allose, d-allose, d-gulose, d-galactose, and l-mannose	IMS-MS; monosaccharide enantiomers were separated by IMS-MS as metal-bound trimeric complexes with an amino acid or short amino acid chain in its L form acting as chiral reference compound	21
Isobaric dipeptides	IMS; crown ethers as shift reagents for non-enatiomeric isobaric dipeptides	22
Bile acids	Separation of Bile acid isomers by formation of cyclodextrin–bile acid host–guest inclusion complex	23
Amino acids	Amino acid enantiomers were separated by FAIMS as metal-bound trimeric complexes with another amino acid in its L form acting as chiral reference compound	24
Amino acids	TWIM-MS; cationisation with copper(II) and multimer formation with D-proline	25
Amino acids	FAIMS; Diastereomeric proton bound complexes were formed between enantiomers of amino acids (analytes) and *N*-*tert*-butoxycarbonyl-*O*-benzyl-l-serine	26
Non enantiomeric glycans	IMS-MS; glycan isomers complexed with different metal cations.	27
Isomeric carbohydrates	Determination of collisional cross sections for four groups of isomeric carbohydrates as their group I metal ion adducts	28

TWIM: traveling wave ion mobility spectrometry.
FAIMS: High-field asymmetric waveform ion mobility.

21. Gaye, M. M.; Nagy, G.; Clemmer, D. E.; Pohl, N. L., Multidimensional Analysis of 16 Glucose Isomers by Ion Mobility Spectrometry. Anal Chem 2016, 88, 2335-44. https://doi.org/10.1021/acs.analchem.5b04280
22. Hilderbrand, A. E.; Myung, S.; Clemmer, D. E., Exploring Crown Ethers as Shift Reagents for Ion Mobility Spectrometry. Anal. Chem. 2006, 78, 6792-800. 10.1021/ac060439v
23. Chouinard, C. D.; Cruzeiro, V. c. W. D.; Roitberg, A. E.; Yost, R. A., Rapid Ion Mobility Separations of Bile Acid Isomers Using Cyclodextrin Adducts and Structures for Lossless

Ion Manipulations. J. Am. Soc. Mass Spectrom. 2017, 28, 323-331. https://doi.org/10.1021/acs.analchem.8b02990
24. Mie, A.; Jornten-Karlsson, M.; Axelsson, B. O.; Ray, A.; Reimann, C. T., Enantiomer Separation of Amino Acids by Complexation with Chiral Reference Compounds and High-Field Asymmetric Waveform Ion Mobility Spectrometry: Preliminary Results and Possible Limitations. Anal. Chem. 2007, 79, 2850-8. https://doi.org/10.1021/ac0618627
25. Domalain, V.; Hubert-Roux, M.; Tognetti, V.; Joubert, L.; Lange, C. M.; Rouden, J.; Afonso, C., Enantiomeric differentiation of aromatic amino acids using traveling wave ion mobility-mass spectrometry. Chem. Sci. 2014, 5, 3234-3239. **https://doi.org/10.1039/C4SC00443D**
26. Zhang, J. D.; Mohibul Kabir, K. M.; Lee, H. E.; Donald, W. A., Chiral recognition of amino acid enantiomers using high-definition differential ion mobility mass spectrometry. Int. J. Mass Spectrom. 2018, 428, 1-7. https://doi.org/10.1016/j.ijms.2018.02.003
Zheng, X., Zhang, X., Schocker, N. S., Renslow, R. S., Orton, D. J., Khamsi, J., ... & Baker, E. S. (2017). Enhancing glycan isomer separations with metal ions and positive and negative polarity ion mobility spectrometry-mass spectrometry analyses. *Analytical and bioanalytical chemistry*, *409*(2), 467-476.
28. Huang, Y.; Dodds, E. D., Ion Mobility Studies of Carbohydrates as Group I Adducts: Isomer Specific Collisional Cross Section Dependence on Metal Ion Radius. Anal. Chem. 2013, 85, 9728-35. https://doi.org/10.1021/ac402133f

Table S2. Resolving power of the IMS instrument for selected peaks of phenylalanine. The average resolving power was 116. These data were calculated with the IMS spectra in Figure 1. The time at which the spectra was taken is shown.

Cation	dt (ms)	B, µl/hr	FWHM	Rp	Time
D-Phe	25.72	10	0.21	122	12:03
L-Phe	25.72	10	0.21	122	12:11
L-Phe	27.12	40	0.34	80	15:39
D-Phe	27.12	40	0.19	143	15:44
D-Phe	27.40	50	0.30	91	16:41
L-Phe	27.40	50	0.20	137	16:49

dt: drift time; B: (S)-2-butanol flow rate; Rp: resolving power; FWHM: full-width at half-maximum. 10 µL/hr = 1.35 mmol m^{-3}

Table S3. ΔK_0' and $\Delta K_{0,c}$ values for experiments in Table 1, reference 12.[12] ΔK_0': percentage mobility difference between enantiomers of the same cation in (S)-2-butanol-doped buffer gas. $\Delta K_{0,c}$: percentage change in K_0 when butanol flow rate was varied, in this case, from 0 to 65 µL/hr into the buffer gas. R = 0.24 and 0.45 for the mass-ΔK_0' and mass-$\Delta K_{0,c}$ correlations, respectively.

Mass	Species	K_0 value in N_2	K_0 in (S)-2-butanol		ΔK_0' %	$\Delta K_{0,c}$ %	
			D-ee	L-ee		D-ee[#]	L-ee*
263.3	Atenolol	1.18	1.18[#]	1.16*	**1.7**	0.0	-1.7
204.2	Tryptophan	1.32	1.25	1.23	*1.6*	-5.3	-6.8
149.2	Methionine	1.56	1.23	1.22	*0.8*	-21.2	-21.8
119.1	Threonine	1.69	1.51	1.48	2.0	-10.7	-12.4
217.2	Methyl α-glucopyranoside[&]	1.30	1.15	1.12	2.6	-11.5	-13.8
203.2	Glucose[&]	1.30	1.23	1.21	*1.6*	-5.4	-6.9
149.2	Penicillamine	1.53	1.42	1.40	*1.4*	-7.2	-8.5
103.2	Valinol	1.74	1.62	1.60	*1.2*	-6.9	-8.0
165.2	Phenylalanine	1.45	1.31	1.28	2.3	-9.7	-11.7
105.1	Serine	1.73	1.55	1.52	1.9	-10.4	-12.1

ee: enantiomer. [#]R-enantiomer for atenolol; *S-enantiomer for atenolol. For example: the value 1.7 of the ΔK_0'of atenolol was calculated as [(1.18-1.16)/1.18]*100 and the value -8.0 of the $\Delta K_{0,c}$ for L- valinol was calculated as [(1.60-1.74)/1.74]*100. Mass: mass of the sodiated[&] (glucose and methyl α-glucopyranoside) or protonated species.

Table S4. Complete version of Table 3 (without atenolol). Here, $\frac{\Delta K_{0,c}}{\overline{\Delta G}}$ was calculated using ΔG of every enantiomer ($\Delta \boldsymbol{G_D}$ and $\Delta \boldsymbol{G_L}$) instead of $\overline{\Delta G}$ and $\Delta K_{0,c}$ average instead of $\Delta K_{0,c}$ of the D-enantiomer; this did not change our results or conclusions. A graphical explanation of this table appears in Figure S9.

Mass	**Species**	$\boldsymbol{K_0}$ **value in N_2**	**Drift time in (S)-2-butanol, ms**		$\boldsymbol{K_0}$ **in (S)-2-butanol**		$\boldsymbol{\Delta K_0}$**' %**	**%$\boldsymbol{\Delta K_{0,c}}$**		$\boldsymbol{\Delta K_{0,c}}$ **average**	$\boldsymbol{\overline{\Delta\Delta G}}$	$\boldsymbol{\Delta G_L}$	$\boldsymbol{\Delta G_D}$	$\boldsymbol{\frac{\Delta K_{0,c}}{\Delta G_D} *}$	$\boldsymbol{\frac{\Delta K_{0,c} *}{\Delta G_L}}$	$\boldsymbol{\frac{\Delta K_0'}{\overline{\Delta\Delta G}}}$
			D-ee	**L-ee**	**D-ee**	**L-ee**		**D-ee**	**L-ee**							
104	Valinol	1.74	18.26	17.84	1.60	1.62	*-1.2*	-8.0	-6.9	-7.47	-1.8	-12.3	-13.4	0.56	0.61	0.69
106	Serine	1.73	18.72	19.11	1.55	1.52	-1.9	-10.4	-12.1	-11.3	-1.7	-23.2	-22.1	0.51	0.49	1.14

ee: Enantiomer. ΔK_0': percentage mobility difference between enantiomers of the same cation in (S)-2-butanol-doped buffer gas. $\Delta K_{0,c}$: percentage change in K_0 when the butanol flow rate was varied. $\overline{\Delta\Delta G}$: average of the complex stabilitiy differences of the R- and S-enantiomers of the same cation with (S)-2-butanol obtained with both functionals in Table 2. $\Delta \boldsymbol{G_D}$ and $\Delta \boldsymbol{G_L}$: Gibbs free energy of the complex formation reactions for enantiomers D- and L-, respectively, in Table 2. The 1.2 value for ΔK_0' of valinol (in italics) was calculated as [(1.60-1.62)/1.62]x100; -6.9 for $\Delta K_{0,c}$ of L-valinol as [(1.62-1.74)/1.74]x100; 1.8 as the mean of $\Delta\Delta G$ values -1.4 and -2.2 in Table 2; 0.54 as -6.9/-12.8; and 0.69 as -1.2/-1.8. * Average

Table S5. Chiral experiments with D and L phenylalanine. (R)-1-phenyl ethanol was used as chiral selector between 0 and 11 mmol m^{-3} at 175°C. The differences were too small to allow the observation of individual peaks when analyzing a racemic mixture with the resolution of the instrument.

(R)-1-phenyl ethanol, mmol m^{-3}	**L-Phe**	**n**	**D-Phe**	**n**	**Drift time difference (ms)**	**Significance level**
0	23.63±0.02	3	23.64±0.02	4	0.01	-
5.3	24.83±0.02	8	24.75±0.03	4	0.08	P = 0.0002
7.9	25.12±0.00	4	25.05±0.01	4	0.07	P = 0.0001
11	25.35±0.04	4	25.28±0.02	8	0.07	P = 0.002

The values were obtained in the following order: 23.63, 23.64, 24.83, 24.75, 25.05, 25.12, 25.04 (repetition of the 25.05 measurement); 25.28, 25.35, 25.26 (repetition of the 25.28 measurement).

Table S6. Drift times of valine enantiomers over an 8-hr period using (S)-2-butanol chiral selector. Solutions of D- valine (■), L- valine (◊) and racemic mixtures of valine (Δ) at a 943-µM concentration were analyzed when 0.69 mmol m^{-3} (S)-2-butanol was introduced into the buffer gas at 150 °C. The drift times were different for both enantiomers (mean drift time separation of ~0.3 ms) but the racemic mixtures yielded only one peak, with a drift time similar to that of D-valine. Variations in drift time for every enantiomer were caused mainly by changes in atmospheric pressure. The drift times of the enantiomers were statistically different ($P<0.05$). The data for this table are plotted in figure A1 in Appendix 1.

Cation	RSD	dt	SD	n	Experiment sequence
L	0.103	19.42	0.02	4	1°
D	0.156	19.23	0.03	10	2°
L	0.102	19.53	0.02	7	3°
D	0.104	19.20	0.02	5	4°
D/L	0.208	19.26	0.04	3	5°
L	0.205	19.50	0.04	6	6°
D	0.207	19.30	0.04	6	7°
L	0.153	19.58	0.03	4	8°
D	0.149	19.42	0.03	5	9°
D/L	0.157	19.16	0.03	4	10°
L	0.206	19.41	0.04	5	11°
D	0.208	19.22	0.04	5	12°
L	0.103	19.38	0.02	5	13°

dt: drift time, ms; SD: standard deviation; n: number of experiments

Table S7. Effect of chiral selector concentration on the mobilities of valinol enantiomers at 125 and 200°C. 943-µM solutions of D-valinol (□), L-valinol (◊) and racemic mixtures (**Δ**) of valinol were analyzed at a buffer gas temperature of 125 °C and 200 °C. At 125°C, the enantiomers had the same drift time but the racemic mixture always yielded a single peak. At 200°C, the enantiomers had the same drift time because the valinol-(S)-2-butanol interaction decreased by the weak analyte-ligand bonds at high temperature and the difference in drift time between the enantiomers was too small. The drift times were statistically different ($P<0.05$) when (S)-2-butanol was introduced at 125°C (bold text). The data for this table are plotted in Figure A2 in Appendix 2.

125°C	**Drift time**					
(S)-2-butanol mmol/m^{-3}	**D-Valinol**	**L-Valinol**	**Average SD**	**n**	**dt-D/L-Valinol**	**n**
0	20.21	20.21	0.04	5		
0.4	**21.49**	**21.89**	0.03	8	21.54	4
1.7	**23.60**	**23.91**	0.02	6	24.26	5
3.4	**24.25**	**24.48**	0.04	6		
5.1	**24.63**	**24.79**	0.05	8		
6.8	**24.80**	**25.00**	0.04	5		
200°C						
(S)-2-butanol mmol/m^{-3}	**D-Valinol**	**L-Valinol**	**Average SD**	**n**	**dt-D/L-Valinol**	**n**
0	17.20	17.21	0.03	4		
0.4	17.24	17.24	0.03	5	17.25	5
1.7	17.27	17.27	0.04	7	17.26	4
3.4	17.29	17.29	0.02	3		
5.1	17.30	17.29	0.03	4	17.30	3
6.8	17.30	17.30	0.02	6		

dt: drift time, ms; SD: standard deviations for D and L enantiomers; n: number of experiments. Mobilities were measured for both enantiomers alternating between the R and S species.

APPENDIX 1. ***Stability of the mobilities of valine enantiomers with time***

The stability of the mobilities of valine enantiomers with time was monitored while injecting (S)-2-butanol in the buffer gas. In one experiment (Figure A1), the drift time of valine enantiomers and racemic mixtures of valine with 0.69 mmol m^{-3} of (S)-2-butanol in the buffer gas was monitored over a period of 8 hours. The drift times of the enantiomers showed a small difference of ~0.15-0.3 ms between the enantiomers, too small to observe their individual peaks in a mixture according to the resolving power of the mobility spectrometer (~100, Figure S4). Additionally, the racemic mixtures yielded only one peak (experiments 2 and 3). However, in several other experiments this behavior was not observed (Table 1).

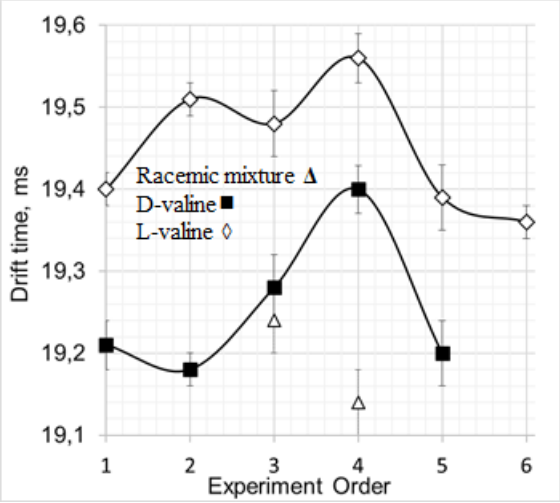

Figure A1. Drift times of valine enantiomers over an 8-hr period using 0.69 mmol m^{-3} of (S)-2-butanol chiral selector. Solutions of D-valine (■), L-valine (◊) and racemic mixtures of valine (Δ) at a 943-µM concentration were analyzed at 150 °C. The racemic mixtures yielded only one peak. Table S6 shows these data. Data were obtained in the SIM-IMS mode selecting the mass of protonated valine. The analyses were made by switching between the D and L enantiomers of valine. The drift times variation was caused mainly by atmospheric pressure drift.

APPENDIX 2. ***Chiral selector concentration and enantiomer separation***

Figure A2 shows that when the chiral selector concentration increased from 0 to 6.8 mmol m^{-3}, the drift times of valinol enantiomers at 125 °C increased. Although there was always a drift time difference between both enantiomers (average ~0.26 ms), only one peak was obtained with the racemic mixture. At 200°C, the mobility of valinol ions was unaffected by increasing the chiral selector concentration in the buffer gas because valinol-(S)-2-butanol electrostatic interactions decreased probably due to weak analyte-ligand bonds at high temperature.

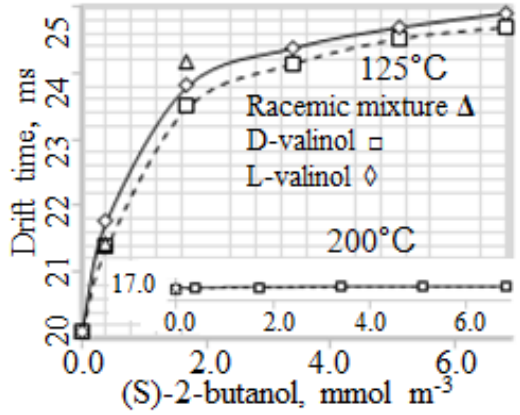

Figure A2. Effect of chiral selector concentration on the mobilities of 943-µM solutions of valinol enantiomers. At 200°C, the enantiomers had the same drift time because the valinol-(S)-2-butanol interaction was decreased by the weak analyte-ligand bonds at high temperature and the drift time difference between the enantiomers was too small. Other experimental conditions were as in Figure A1 in Appendix 1. See Table S7 for drift time values.

The formation of large valinol-(S)-2-butanol clusters (*m/z* 178, Figure S10) explains the increase of valinol drift time from ~20 to ~25 ms (Figure A4) when (S)-2-butanol was introduced into the buffer gas. The intensity of the valinol cluster peak at *m/z* 178 increased with respect to that of the protonated peak of D-valinol at *m/z* 104 (Figure S10) when the chiral selector concentration increased from 2.8 to 4.1 mmol m^{-3}, as expected if the cluster was formed from protonated valinol. Figure S10 also illustrates the expected increase in peak intensity of the dimer (B_2H^+, *m/z* 149) and trimer (B_3H^+, *m/z* 223) of (S)-2-butanol when the chiral selector concentration was increased.

APPENDIX 3. ***Buffer gas temperature and separation of valinol enantiomers***

Figure A3 shows the drift time of valinol enantiomers and racemic mixtures of valinol when the buffer gas temperature was varied from 125 to 200°C at a 0.28 mmol m^{-3} concentration of (S)-2-butanol. The enantiomer drift times were not significantly different. Again, the racemic mixtures yielded only one peak. This lack of separation was probably due to an insufficiente drift time separation between the enantiomers compared to the resolving power of the instrument or drift time time differences between the enantiomers produced by chance..

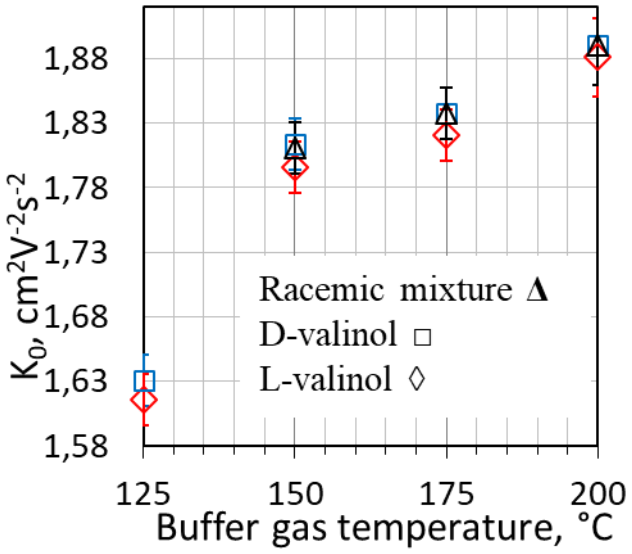

Figure A3. Effect of temperature on the mobilities of valinol enantiomers and racemic mixtures of 943-µM valinol solutions. (S)-2-butanol: 0.28 mmol m^{-3}. The drift time differences between the enantiomers were not statistically significant as shown by the error bars. The racemic mixtures yielded only one peak. Other experimental conditions were were those in Figure A1, Appendix 1.

APPENDIX 4. ***Analyte concentration and enantiomer separation***

Figure A4 shows the drift times of solutions of 10-, 50-, 250-, and 943-µM solutions of D- and L-valinol, and of racemic mixtures of valinol enantiomers with 0.69 mmol m^{-3} of (S)-2-butanol in the buffer gas at 150 °C. The effect of valinol concentration was not important on the mobilities of its enantiomers when (S)-2-butanol was introduced into the buffer gas under the experimental conditions. The drift times of valinol enantiomers were slightly different (0.15-0.35 ms in average), but the racemic mixture produced only a single peak, with a drift time similar to that of D-valinol. Variations in drift time were caused mainly by changes in atmospheric pressure and other instrumental parameters. Other experimental conditions were as in Appendix 1. As before, the drift times of valinol enantiomers were significantly different (0.3 ms average) However, several experiments at different instrumental conditions were unsuccessfully tested for enantiomer separation: 50-, 250- and 1000-µM serine, atenolol, and glucose at 0.28, 0.55, 0.83, and 1.1 mmol m^{-3} (S)-2-butanol with several repetitions at different times; D- and L-valinol at 10, 50, 250, and 943 µM and 250 and 943-µM racemic mixtures of valinol with 0.75 mmol m^{-3} (S)-2-butanol at 150 °C (Table 1).

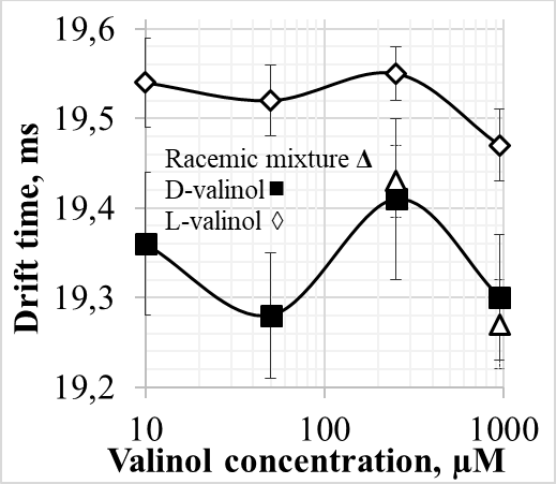

Figure A4. **Effect of valinol concentration on the mobilities of its enantiomers.** Solutions of D-valinol (■) and L-valinol (◊)were analyzed at concentrations of 10, 50, 250, and 943 µM (logarithmic scale) and racemic mixtures (Δ) of valinol at concentrations of 250 and 943 µM when 0.75 mmol m^{-3} of (S)-2-butanol was introduced into the buffer gas at 150 °C.

APPENDIX 5. ***Claimed separation of fluoxetine enantiomers***

Regarding the separation of fluoxetine enantiomers (Figure S2) using (S)-2-butanol reported by Karas in a patent,[13] it is not clear how such a large molecule (309.3 g/mol) can yield such a large separation and drift. We have studied atenolol, a smaller molecule with 266.3 g/mol, also an amino compound, by injecting 2-butanol in the buffer gas and a saturation of the binding sites with butanol molecules on this analyte has been reached before 6.8 mmol m^{-3} 2-butanol. This saturation is expressed as a stabilization of the mobility of atenolol with higher concentrations of 2-butanol because no additional molecules of 2-butanol can attach to atenolol. This attachment is what produces the mobility shifts in IMS. For atenolol, we obtained a $\Delta K_{0,c}$ (percentage change in K_0 when the dopant concentration was varied) of only -0.7%. From the data in the patent, a 16.2 ms drift time in pure nitrogen buffer gas and 19.52 ms after adding 2-butanol at 5 mol% (molar fraction), a $\Delta K_{0,c}$ of 20.7% can be calculated with a molecule larger than atenolol. With a larger size, fluoxetine should yield a smaller $\Delta K_{0,c}$ than that of atenolol, -0.7%, because size decreases the effect of buffer additives on mobilities.[20] In support of this discussion, even reference 12 found a $\Delta K_{0,c}$ of 0.0% for the (R)-atenolol enantiomer, as expected.[12] However, patents are not peer-reviewed and, therefore, its claims have not been verified.

APPENDIX 6. ***Recommendations for potential enantiomer separations***

- Chiral separations in IMS might be obtained with small chiral analytes and large chiral selectors. The mobility of small analytes is more affected by chiral interactions than that of large analytes and large selectors decrease the mobility of ions more than small ones.
- The type of chiral interactions between selectors and analytes must be strong, of the polar type, so that the difference between two-points and three-points interactions is large.
- In some cases, there should be as many strong potential interactions as possible. For this reason, serine would be preferable as an analyte to valine since the former has three groups to interact, amino, alcohol, and carboxylic, and valine only amino and alcohol groups.
- The buffer gas temperature should be low enough to allow these interactions.[19] This has to do with the formation of clusters, which slow down the ions and are absent at high temperatures (Figure S10). If enantiomer separation of amino acids is not obtained before the flattening of the curve of chiral selector concentration vs. mobilities of enantiomers (Figure A2, Appendix 2), it is unlikely that separation will be obtained at larger chiral selector flow rates because saturation of the ion with chiral selector molecules will prevent the chiral interaction.
- Water and contamination must be kept out of the drift tube. They cluster with the analyte deforming the chiral sites and obscuring chiral interactions.

Graphical abstract

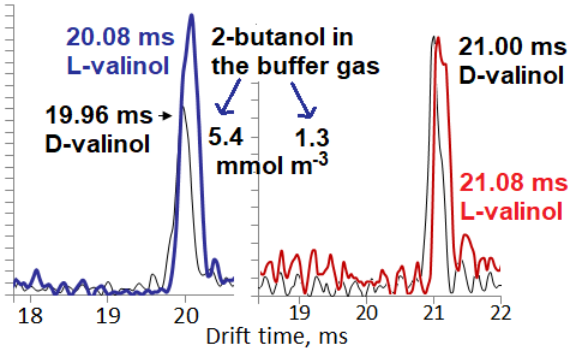

Not enough resolution to separate enantiomers by drift tube IMS

Highlights

- Racemic mixtures were tested for enantiomer separation by ion mobility spectrometry (IMS)- mass spectrometry
- Chiral selectors were volatilized into the mobility instrument buffer gas
- Experimental conditions were varied trying to find the best separation conditions
- The individual enantiomers yielded different drift times in some experiments, different enough to resolve the enantiomers in racemic mixtures, but mixtures did not separate
- Chiral selector–ion free energies showed that these separations are unlikely using 2-butanol as selector

SIGNIFICANCE STATEMENT

We demonstrate that enantiomers cannot be separated by drift tube Ion Mobility Spectrometry (DTIMS) as reported by Dwivedi et al. (2006).[1] We unsuccessfully tested racemic mixtures of fifteen chiral compounds for enantiomer separation by introducing seven chiral selectors in DTIMS in more than 4000 experiments. Energy calculations of the chiral selector –ion interactions show that these separations are unlikely using 2-butanol as a chiral selector.

Several plausible explanations for the lack of success, a critical review of claimed enantiomer separations by DTIMS, and recommendations for potential separations by DTIMS are included.